LEVEL II

ASL-CR-79-0100-4

AD

Reports Control Symbol
OSD 1366

ATMOSPHERIC EFFECTS ON THE SPEED OF SOUND

August 1979

Prepared by
E.A. DEAN
Physics Department
University of Texas at El Paso
El Paso, Texas 79968

Under Contract: DAAG29-76-D-0100
Delivery Order No. 1206 (TCN 79-147)
Battelle Columbus Laboratories
Contract Monitor: ABEL J. BLANCO

Approved for public release; distribution unlimited

US Army Electronics Research and Development Command
ATMOSPHERIC SCIENCES LABORATORY
White Sands Missile Range, NM 88002

NOTICES

Disclaimers

The findings in this report are not to be construed as an official Department of the Army position, unless so designated by other authorized documents.

The citation of trade names and names of manufacturers in this report is not to be construed as official Government indorsement or approval of commercial products or services referenced herein.

Disposition

Destory this report when it is no longer needed. Do not return it to the originator.

SECURITY CLASSIFICATION OF THIS PAGE (When Data Entered)

REPORT DOCUMENTATION PAGE

READ INSTRUCTIONS BEFORE COMPLETING FORM

1. REPORT NUMBER: ASL-CR-79-0100-4

2. GOVT ACCESSION NO.:

3. RECIPIENT'S CATALOG NUMBER:

4. TITLE (and Subtitle): ATMOSPHERIC EFFECTS ON THE SPEED OF SOUND

5. TYPE OF REPORT & PERIOD COVERED: Technical Report

6. PERFORMING ORG. REPORT NUMBER:

7. AUTHOR(s): E. A. Dean

8. CONTRACT OR GRANT NUMBER(s): DAAG29-76-D-0100

9. PERFORMING ORGANIZATION NAME AND ADDRESS:
Physics Department
University of Texas at El Paso
El Paso, Texas 79968

10. PROGRAM ELEMENT, PROJECT, TASK AREA & WORK UNIT NUMBERS:
DA Task No. 1L162111AH71 26

11. CONTROLLING OFFICE NAME AND ADDRESS:
US Army Electronics Research
and Development Command
Adelphi, MD 20783

12. REPORT DATE: August 1979

13. NUMBER OF PAGES: 53

14. MONITORING AGENCY NAME & ADDRESS (if different from Controlling Office):
Atmospheric Sciences Laboratory
White Sands Missile Range, NM 88002

15. SECURITY CLASS. (of this report): UNCLASSIFIED

15a. DECLASSIFICATION/DOWNGRADING SCHEDULE:

16. DISTRIBUTION STATEMENT (of this Report): ERADCOM/ASL

19. CR-79-0100-4

Approved for public release; distribution unlimited

17. DISTRIBUTION STATEMENT (of the abstract entered in Block 20, if different from Report)

18. SUPPLEMENTARY NOTES

Contract Monitor: Abel J. Blanco

Delivery order no. 1206 (TCN 79-147)

19. KEY WORDS (Continue on reverse side if necessary and identify by block number)

Sound ranging
Atmospheric propagation
Meteorological corrections
Frequency of speed of sound

20. ABSTRACT (Continue on reverse side if necessary and identify by block number)

The small-signal speed of sound in humid air is calculated from a model which includes the real-gas effects from the equation of state for humid air and the vibrational dispersion due to N_2, O_2, and CO_2 relaxation. Other atmospheric effects such as dispersion due to viscothermal and rotational relaxation, heat radiation, propagation along the air-ground boundary, the density gradient, turbulence, aerosols and fogs are considered and found to be unimportant for frequencies between 1 Hz and 5 MHz (at one atmosphere). The uncertainty in

DD FORM 1 JAN 73 1473 EDITION OF 1 NOV 65 IS OBSOLETE

391 859

SECURITY CLASSIFICATION OF THIS PAGE (When Data Entered)

20. ABSTRACT (cont)

predicting the sound speed varies between 0.22 m/sec at -90°C to 0.05 m/sec at 90°C. Experimental results in humid air at 20°C and 30°C are in excellent agreement with the model. For the propagation frequency of 20 Hz, it is found that the presently used sound-ranging formula, $c = 20.06\sqrt{T_s}$, where $T_s = .75t_v + .25t + 273.2$ (t_v = virtual temperature), differs by up to 0.5 m/sec over the range -60°C to 60°C. A correction to the "sonic" temperature determination is suggested which results in deviations of less than 0.05 m/sec over the temperature range from -60°C to 50°C and for relative humidities from 5% to 100%.

TABLE OF CONTENTS

Introduction	1
Ideal-gas speed of sound	3
Real-gas corrections	9
Dispersion corrections	17
Comparison of models	32
Experimental results	43
Other atmospheric effects	47
Summary and recommendations	50
References	52

LIST OF TABLES

1. Mole fractions, non-vibrational molar heat capacities, and molar masses of primary components of air. 5

2. Recent determinations of the gas constant. 6

3. Second virial coefficients for moist air. 11

4. Coefficients for the real-gas correction to the speed of sound in moist air. 12

5. Recent determinations of relaxation times due to CO_2 collisions. 24

6. Uncertainties in the theoretical calculation of sound speed. 35

LIST OF FIGURES

1. Ratio of ideal-gas sound speed with mole fraction water vapor. 8

2. The real-gas correction to the sound speed. 13

3. Real-gas sound speed correction factor vs. relative humidity at various temperatures. 15

4. The quantity ϵ in $c = c_a (1 + \epsilon x)$, where c_a is the real-gas sound speed for dry air. 16

5. Contributions of vibrational specific heats to the sound speed vs. temperature. 22

6. Temperature dependence of CO_2-induced relaxation. 25

7. Dispersion for 20°C. 28

8. Sound speed correction for 20 Hz and various temperatures and low relative humidities. 30

9. Sound speed correction at 20 Hz for various temperatures up to 100% R.H. 31

10. Differences in sound speed for various models. 34

11. Difference between theory and $c = 20.06 \sqrt{T_s}$, where $T_s = t + .8\Delta t + 273.0$. 37

12. Difference between theory and $c = 20.06 \sqrt{T_s}$, where $T_s = t + .825\Delta t - 1 \times 10^{-3}\ t - 6 \times 10^{-5}\ t^2 + 273.0$ 38

13. Difference between theory and approximation given by Eq. (1) and (73). Pressure variation. 40

14. Difference between theory and approximation given by Eq. (1) and (73). Frequency variation at 50% R.H. 41

15. Difference between theory and approximation given by Eq. (1) and (73). Frequency variation at 5% R.H. 42

16. Experimental results for sound speed in humid air at 20°C. 44

17. Experimental results for the speed of sound in humid air at 30°C. 46

Atmospheric Effects on the Speed of Sound

INTRODUCTION

For sound ranging, the speed of sound acts as a scale factor which transforms the measured time differences at the microphones into distance to the source. Thus an error of 0.1% in the speed of sound results in a distance error of 0.1%, or 100 m in 10 km. The errors due to the vagaries of the meteorological parameters over such a path length may be larger than this, but, with the proper model, tend to be random and cancel in the long run. This is not so for the systematic errors introduced by an inaccurate speed of sound scale factor. Because of the systematic and sensitive nature of sound speed errors, it is important that this quanity be known accurately as a function of meteorological parameters.

The formula used to determine the speed of sound for sound-ranging purposes is[1]

$$c = 20.06\ (T_s)^{1/2}, \tag{1}$$

where c is the sound speed and T_s is the absolute sonic temperature, defined by

$$T_s = \frac{3t_v + t}{4} + 273.2\ , \tag{2}$$

where t_v is the virtual temperature and t is the dry-bulb temperature, both measured in ^{o}C. The goal of this investigation is to ascertain the validity of Eq. (1) and Eq. (2) over the ranges of temperature, humidity, and pressures likely to be encountered in sound ranging.

For an ideal gas, the sound speed is a function of the temperature and composition of the gas. For a real gas, the equation of state introduces a correction which is a function of temperature, pressure, and composition. In addition, the effective specific heats of a polyatomic gas depend on the fre-

quency of the sound wave because of vibrational relaxation phenomena. After a review of the above theory, a comparison of the theory with the present formula and with laboratory determinations of the speed of sound in air will be made. This will be followed by considering other effects peculiar to the atmosphere and a summary with recommendations.

IDEAL - GAS SPEED OF SOUND

The linear theory (small-signal theory) of sound propagation in fluids yields

$$c^2 = \left(\frac{\partial p}{\partial \rho}\right)_S , \tag{3}$$

where p is the pressure, ρ is the density, and the subscript S denotes that the derivative is to be taken with the entropy held constant (adiabatic propagation). Standard thermodynamic manipulation yields

$$c^2 = \frac{C_p}{C_v \rho k} , \tag{4}$$

where C_p is the molar heat capacity at constant pressure,

$$C_p = T\left(\frac{\partial S}{\partial T}\right)_p , \tag{5}$$

C_v is the molar heat capacity at constant volume,

$$C_v = T\left(\frac{\partial S}{\partial T}\right)_V , \tag{6}$$

and k is the isothermal compressibility,

$$k = -\frac{1}{V}\left(\frac{\partial V}{\partial p}\right)_T , \tag{7}$$

In the above and succeeding discussion, the extensive thermodynamic variables such as entropy S and volume V are per mole.

Equation (4) is correct for any fluid. For an ideal gas,

$$pV = RT, \tag{8}$$

where R is the universal gas constant. Use of Eq. (7) and Eq. (8) and the definition of density yields

$$c^2 = \frac{\gamma RT}{M} , \tag{9}$$

where γ is the ratio of specific heats, C_p/C_v and M is the molar mass (molecular weight). Further, since for an ideal gas

$$C_p - C_v = R \ , \tag{10}$$

Eq. (9) becomes

$$c^2 = \left(1 + \frac{R}{C_v}\right)\frac{RT}{M} \ . \tag{11}$$

Thus, for the ideal-gas approximation, C_v and M are the only two parameters characteristic of the gas required to determine the speed of sound.

For a mixture of ideal gases, the values of C_v and M are

$$C_v = \Sigma\, x_i\, C_i \ , \tag{12}$$

$$M = \Sigma\, x_i\, M_i \ , \tag{13}$$

where x_i, C_i, and M_i are the mole fraction (fractional number of molecules,) the molar heat at constant volume and the molar mass of the ith component respectively. Table 1 lists these quantities for the primary components of air. The molar heats are assumed to be composed of translational and rotational energies where equipartition holds. Since this does not include the non-equipartional vibrational energies, these molar heats are the effective ones for high frequencies where vibrational energy does not reach equlibrium during the passage of the sound wave. Therefore, the superscript ∞ is used. The molar masses are based on the unified atomic mass scale ($^{12}C = 12$).

Thus, in the ideal-gas approximation, the effect of water vapor on the speed of sound is two-fold: (1) an increase due to decreasing the mean molar mass, and (2) a decrease due to increasing the mean molar heat capacity. Since the virtual temperature is defined as that temperature required for dry air to

Table 1. Mole fractions, non-vibrational molar heat capacities, and molar masses of primary components of air.

Component	Mol fraction	C_v^∞/R	M
Nitrogen	0.7809	2.5000	28.0134
Oxygen	0.2095	2.5000	31.9988
Argon	0.0093	1.5000	39.948
Carbon Dioxide	0.0003	2.5000	44.0108
Dry Air		2.4907	28.9641
Water vapor	x	3.0000	18.0152

have the ideal-gas density of moist air at a particular pressure, the absolute virtual temperature is

$$T_v = T \frac{M_a}{M} , \tag{14}$$

where M_a is the molar mass of dry air. Thus the increase in sound speed (effect 1) is characterized by using the virtual temperature rather than the dry-bulb temperature.

The net effect, including effect (2), is presently estimated at 75% of the density effect, which yields Eq. (2). This weighted sonic temperature is based[2] on an expression due to Gutenberg[3,4],

$$c = c_a (1 + 0.14x), \tag{15}$$

where c_a is the sound speed in dry air and x is the mole fraction of water vapor.

To determine the constant in Eq. (1), one must use the gas constant. The value given in the 1973 adjustment to the fundamental constants[5], which includes changes due to the unified atomic mass scale and the 1954 redefinition

of the ice point as 273.150 K, is shown in Table 2; also shown are more recent results. We shall use the 1973 value, 8314.41 ± .26 JK^{-1} $kmol^{-1}$. Furthermore, we will assume a ± .001 expected error for the molar mass due to a ± 50 ppm deviation in CO_2 content and the estimated error for C_v^∞/R of ± .0003. This yields

$$c_\infty^o = (20.0577 \pm .0006)(t + 273.15)^{1/2}, \qquad (16)$$

where the subscript indicates non-vibrational specific heats and the superscript indicates ideal gas, and t is the temperature in ^oC.

Table 2. Recent determinations of the gas constant.

Reference	Value ($J\ K^{-1}\ kmol^{-1}$)	Method
a	8314.41 ± .26	Mean of pre-1962 data
b	8314.33 ± .44	Density (1964)
c	8314.7 ± .5	Density (1965)
d	8315.59 ± .18	Sound speed (1974)
e	8314.79 ± .35	Sound speed (1976)

a. Cohen and Taylor, J. Phys. Chem. Ref. Data 2,663 (1973).
b. Rossini, Pure Appl. Chem. 9, 453 (1964).
c. Din, J. Chem. Soc. London 1965, 829.
d. Quinn, Chandler, and Colclough, Nature 250, 218 (1974).
e. Gammon, J. Chem. Phys. 64, 2556 (1976).

Equation (16) is for dry air. The addition of water vapor changes C_v^∞ and M to

$$C_v^\infty/R = 2.4907\ (1 + 0.2045x), \qquad (17)$$

$$M = 28.9641\ (1-0.3780x), \qquad (18)$$

or

$$T_s = T \frac{1 + 0.1459x}{(1 + 0.2045x)(1-0.3780x)} , \quad (19)$$

where T_s is the effective "sonic" temperature. The binomial expansion of Eq. (19) yields

$$c = c_a (1 + 0.1597x) , \quad (20)$$

which is larger than Gutenberg's result, and represents 84% of the density effect given by the virtual temperature.

The amount of water vapor possible in the atmosphere is normally small so that the linear expansion given in Eq. (20) is probably sufficient. This is shown in Figure 1, where the square root of the coefficient in Eq. (19) is plotted vs. the mole fraction of water vapor. Plots of this nature are used throughout this work. Let us define

$$c = c_o(1 + \delta), \quad (21)$$

such that δ is the fractional difference between the sound speed and some reference sound speed, $\delta = (c - c_o)/c_o$. Thus Fig. 1 is a plot of δ vs x.

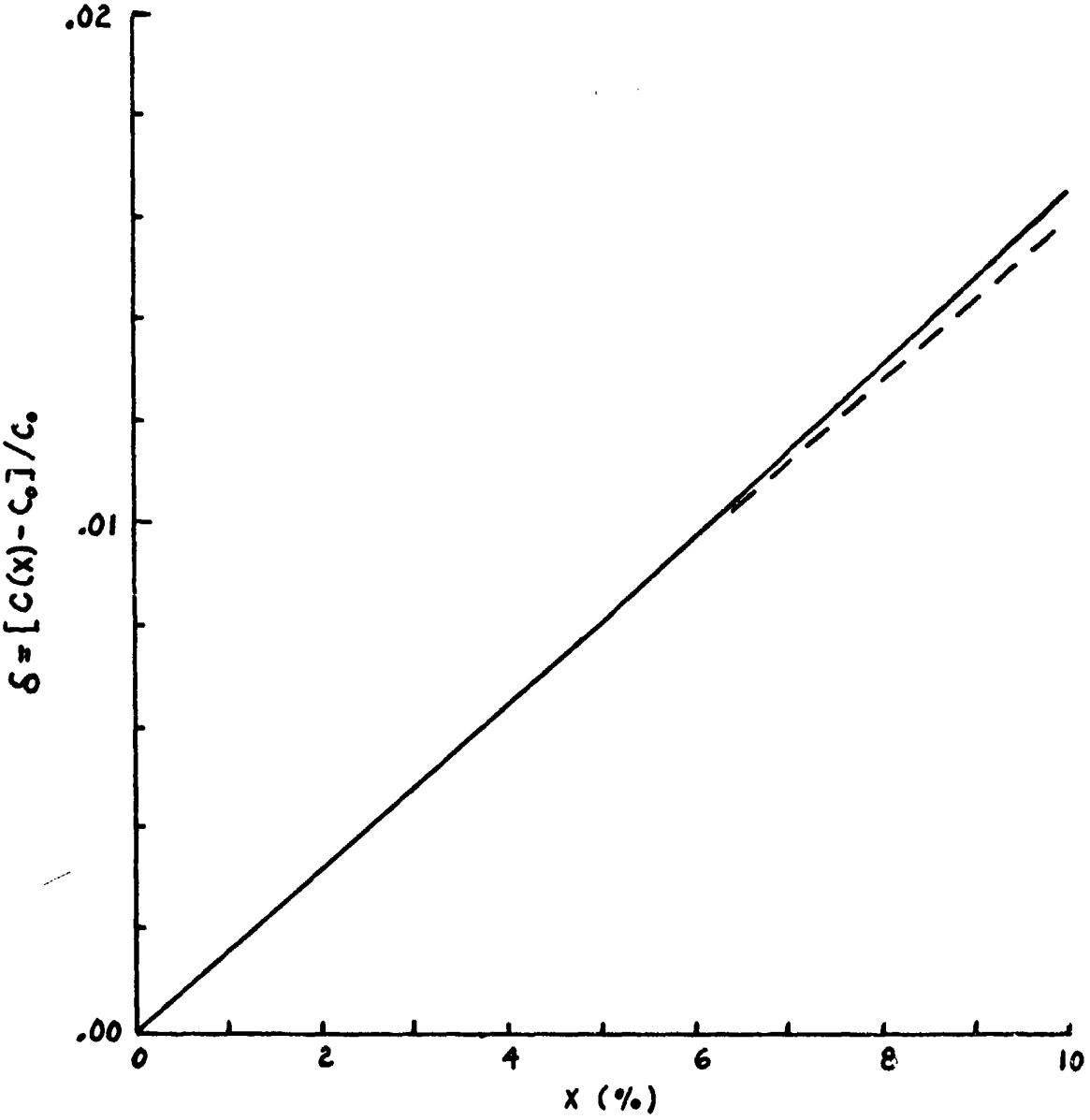

Figure 1. Ratio of ideal-gas sound speed with mole fraction water vapor. The top curve is the ratio, while the bottom curve is the linear expansion 1 + .1597x.

REAL-GAS CORRECTIONS

Air at one atmosphere of pressure deviates slightly from an ideal gas. This deviation results in a correction to the compressibility and both molar heat capacities. In addition, the deviation depends on the amount of water vapor present. The equation of state may be expressed as a virial expansion,

$$\frac{pV}{RT} = 1 + \frac{B}{V} + \ldots, \tag{22}$$

where the first coefficient (unity) is the ideal-gas equation of state, and B is the second virial coefficient. For the small deviations in the atmosphere, the expansion may be terminated with the second virial coefficient, which itself is a function of temperature.

Using Eq. (21), the effect on the speed of sound may be determined as[6]

$$c = c^{o} \left\{ 1 + \frac{p}{RT} \left[B + (\gamma^{o}-1) T \frac{dB}{dT} + \frac{(\gamma^{o}-1)^{2}}{2\gamma^{o}} T^{2} \frac{d^{2}B}{dT^{2}} \right] \right\} , \tag{23}$$

where the superscripts ^{o} denote zero-pressure (ideal-gas) values. For a mixture of two gases, the second virial coefficient is represented by [7]

$$B = (1-x)^{2} B_{1} + 2x(1-x) B_{12} + x^{2} B_{2} , \tag{24}$$

where x is the mole fraction of the second gas, B_1 and B_2 are the second virial coefficients of the first and second gases, and B_{12} is an empirically determined interaction virial coefficient.

The International Joint Committee on Psychrometric Data[8] has recommended the following second virial coefficients for dry air and water vapor:

$$B_{1} = 40.70 - 13116/T - 12 \times 10^{7}/T^{3} , \tag{25}$$

$$B_{12} = 29.53 - .00669\, T[1-\exp(-4416.5/T)] - 17546/T - 95300/T^{2} - 8.515 \times 10^{7}/T^{3} , \tag{26}$$

$$B_2 = 33.97-(55306/T)(10^{72000/T^2}) \quad , \tag{27}$$

where the units of B are $cm^3/gmol$ and $T = t + 273.16$. The differentiation of Eq. (25)-(27) yields the required values TdB/dT and T^2d^2B/dT^2. If the new variables

$$a_0 = B_1 + (\gamma^o-1)T\frac{dB_1}{dT} + \frac{(\gamma^o-1)^2}{2\gamma^o}T^2\frac{d^2B_1}{dT^2} \quad , \tag{28}$$

$$a_1 = 2\left[B_{12} + (\gamma^o-1)T\frac{dB_{12}}{dT} + \frac{(\gamma^o-1)^2}{2\gamma^o}T^2\frac{d^2B_{12}}{dT^2} - a_0\right] \quad , \tag{29}$$

$$a_2 = B_2 + (\gamma^o-1)T\frac{dB_2}{dT} + \frac{(\gamma^o-1)^2}{2\gamma^o}T^2\frac{d^2B_2}{dT^2} - 2a_1 + a_0 \quad , \tag{30}$$

are defined, then

$$c_\infty = c_\infty^o\left[1 + \frac{p}{RT}(a_0 + a_1x + a_2x^2)\right] \tag{31}$$

Table 3 lists the values for B_1, B_{12}, and B_2 as functions of temperature, while Table 4 lists the values of a_0, a_1, and a_2. Division of the a's by RT, where $R = 82.056\ cm^3\ atm\ gmol^{-1}\ K^{-1}$, yields

$$c_\infty = c_\infty^o[1 + p^*(b_o + b_1x + b_2x^2)] \quad , \tag{32}$$

where the b's may be expressed by the following polynomial regressions,

$$b_o = \frac{a_o}{RT} = 0.445/T - 76.7/T^2 - 3950/T^3 \quad , \tag{33}$$

$$b_1 = \frac{a_1}{RT} = -0.481/T \quad , \tag{34}$$

$$b_2 = \frac{a_2}{RT} = -\frac{.01219}{T}\exp(1.91 + 960/T + 1.77 \times 10^5/T^2), \tag{35}$$

and p^* is the pressure expressed in atmospheres.

A plot from -60^oC to 60^oC of $b_o + b_1x + b_2x^2$ is shown in Fig. 2. The various curves at the higher temperatures are for 0%, 25%, 50%, 75%, and 100% relative humidity (R.H.). The mole fractions were calculated from [9].

Table 3. Second virial coefficients for moist air. Taken from Goff[7].

T (°C)	B_1 (cm^3/gmol)	B_{12} (cm^3/gmol)	B_2 (cm^3/gmol)
-90	-50.4 ± 3.9	-84.2 ± 8.6	
-80	-43.9 ± 3.3	-77.0 ± 8.2	
-70	-38.2 ± 2.9	-70.7 ± 7.8	
-60	-33.2 ± 2.5	-65.1 ± 7.5	
-50	-28.9 ± 2.2	-60.2 ± 7.2	
-40	-25.0 ± 1.9	-55.8 ± 7.0	
-30	-21.6 ± 1.7	-51.8 ± 6.7	
-20	-18.5 ± 1.5	-48.2 ± 6.5	
-10	-15.7 ± 1.3	-45.0 ± 6.3	-2300 ± 1900
0	-13.2 ± 1.2	-42.0 ± 6.1	-1830 ± 800
10	-10.9 ± 1.1	-39.3 ± 6.0	-1510 ± 400
20	- 8.8 ± 1.0	-36.8 ± 5.8	-1260 ± 210
30	- 6.9 ± 0.9	-34.5 ± 5.7	-1074 ± 116
40	- 5.1 ± 0.8	-32.3 ± 5.5	- 924 ± 66
50	- 3.4 ± 0.7	-30.4 ± 5.4	- 803 ± 40
60	- 1.9 ± 0.6	-28.5 ± 5.3	- 705 ± 25
70	- 0.5 ± 0.6	-26.8 ± 5.2	- 625 ± 16
80	+ 0.8 ± 0.5	-25.2 ± 5.1	- 558 ± 10
90	+ 2.1 ± 0.5	-23.7 ± 5.0	- 501 ± 7

Table 4. Coefficients for the real-gas correction to the speed of sound in moist air. $c = c^o[1 + (p/RT)(a_o + a_1x + a_2x^2)]$.

T (^oC)	a_o ($cm^3/gmol$)	a_1 ($cm^3/gmol$)	a_2 ($cm^3/gmol$)
-90	-19.9 ± 11.7	-41 ± 32	
-80	-15.7 ± 9.5	-41 ± 28	
-70	-12.1 ± 7.9	-42 ± 26	
-60	- 9.1 ± 5.4	-40 ± 22	
-50	- 6.6 ± 5.4	-40 ± 20	
-40	- 3.9 ± 4.8	-41 ± 20	
-30	- 1.8 ± 4.2	-40 ± 19	
-20	0.2 ± 3.7	-40 ± 16	
-10	2.1 ± 3.2	-40 ± 16	-3400 ± 2200
0	3.7 ± 3.1	-40 ± 15	-2450 ± 1060
10	5.0 ± 2.7	-38 ± 15	-1850 ± 530
20	6.4 ± 2.5	-40 ± 15	-1410 ± 290
30	7.6 ± 2.2	-38 ± 14	-1106 ± 158
40	9.0 ± 2.1	-38 ± 14	- 887 ± 91
50	9.9 ± 2.0	-37 ± 12	- 721 ± 55
60	11.0 ± 1.7	-39 ± 12	- 595 ± 35
70	11.9 ± 1.6	-39 ± 12	- 500 ± 24
80	12.7 ± 1.6	-37 ± 12	- 426 ± 18
90	13.9 ± 1.5	-39 ± 12	- 365 ± 15

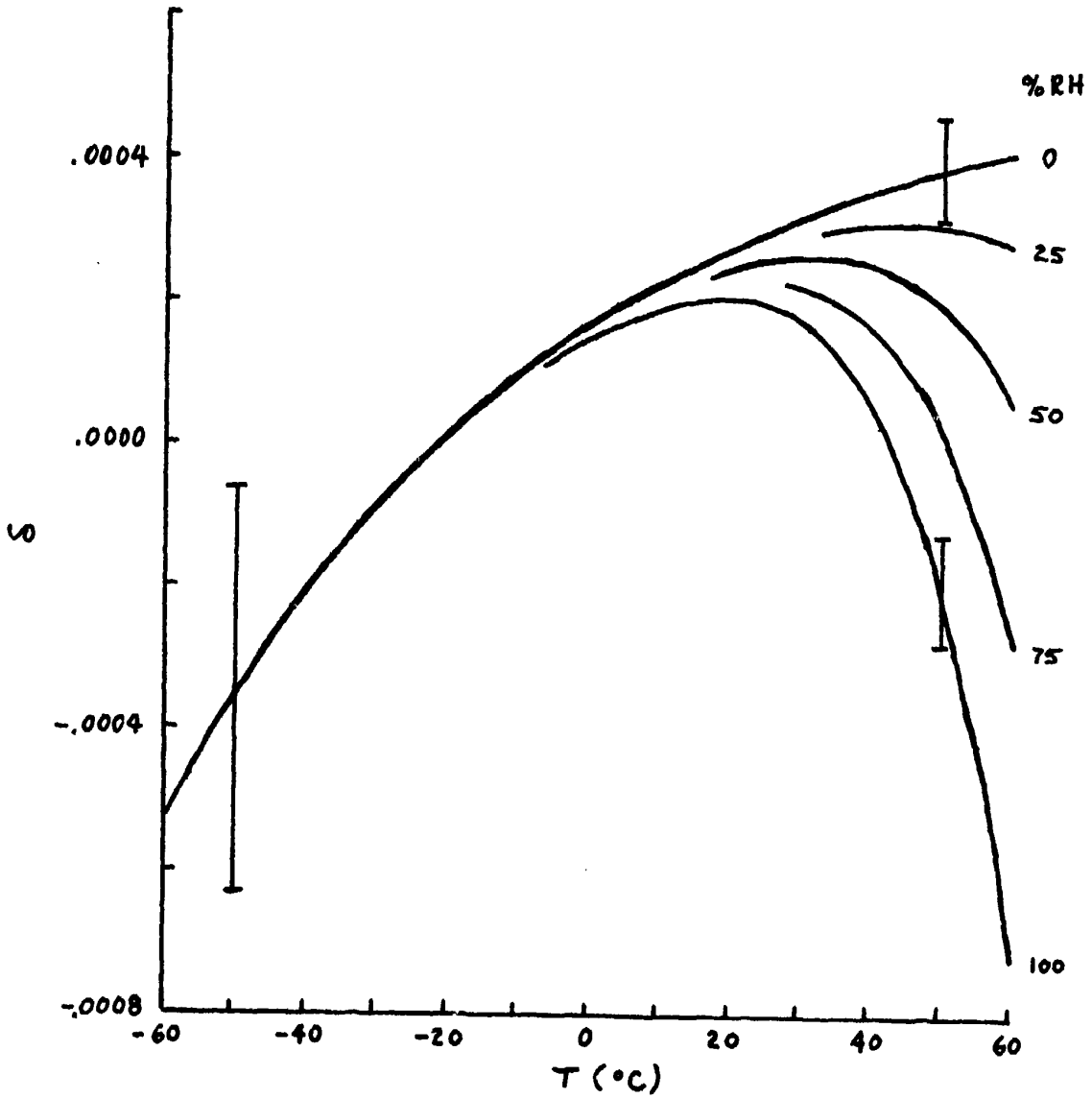

Fig. 2. The real-gas correction to sound speed.

$$\log_{10} x_s = 20.5318 - 2939/T - 4.922 \log_{10} T, \quad (36)$$

where x_s is the saturated mole fraction. The error bars at $-50^{o}C$ and $50^{o}C$ indicate the uncertainty in the equation of state correction. Even though the equation of state correction has a negative term that depends on the square of the humidity, the correction is small compared to the density-specific heat correction (Eq. (19)) and the effect on sound speed is still almost linear for a real gas. This is shown in Fig. 3, where δ is plotted vs relative humidity for various temperatures. The dotted line represents the ideal-gas, dry-air speed.

Since the effect of humidity is so nearly linear, one may use

$$c = c_a (1 + \theta x) . \quad (37)$$

A plot of θ vs T is shown in Fig. 4. Here θ is determined by $(c(x_s)-c(o))/c_o x_s$. It is noted that θ for the real gas is different from that of the ideal gas, represented by the dotted line. At low temperatures, the equation of state correction reduces θ due to the large value of a_2, whereas for high temperatures a_2 is smaller and the non-linear portion of Eq. (19) increases θ. It may be noted that Gutenberg's θ (.14) is off scale.

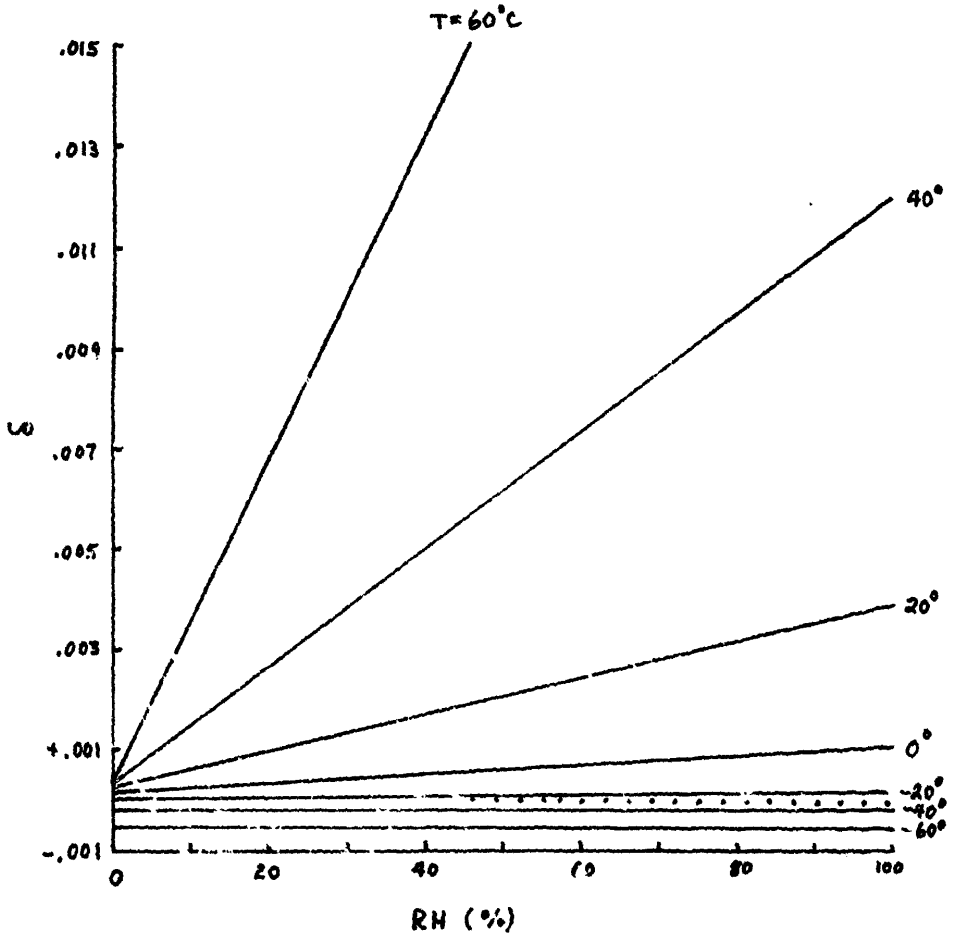

Fig. 3. Real-gas sound speed correction factor vs. relative humidity at various temperatures.

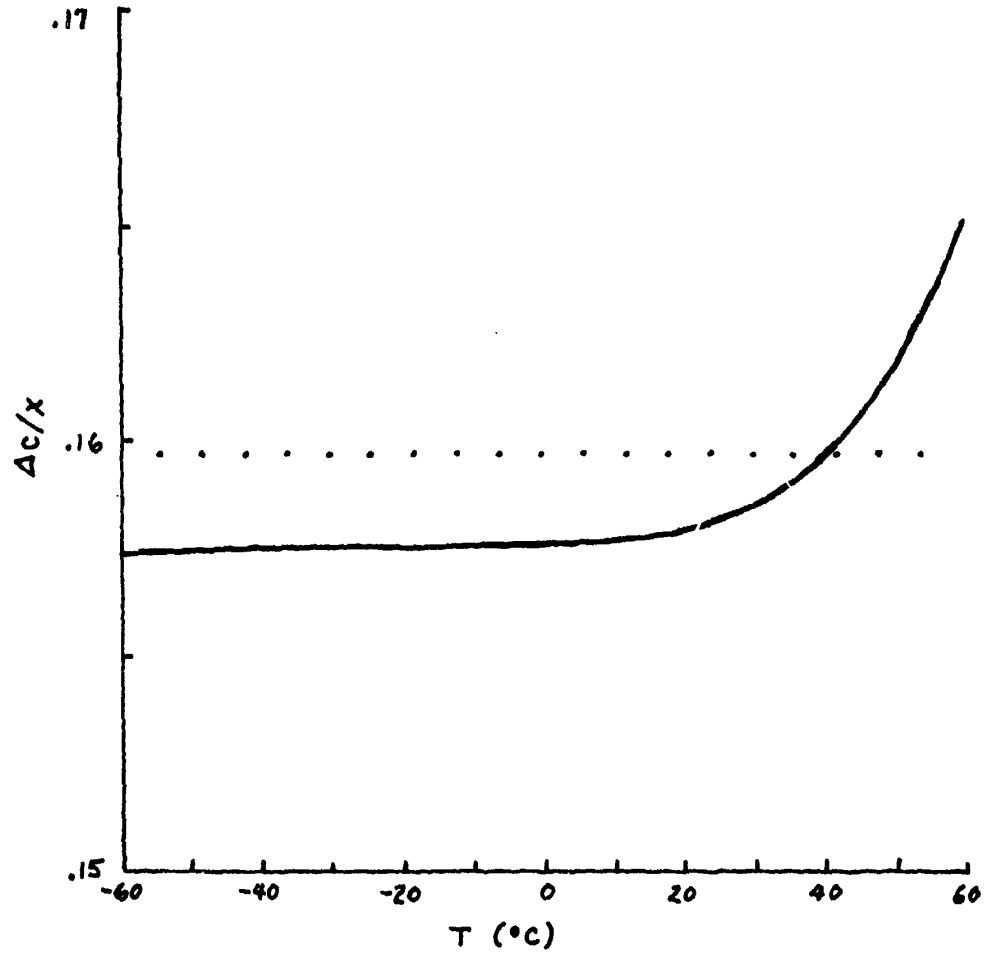

Fig. 4. The quantity 6 in $c = c_a(1 + 6x)$ where c_a is the real-gas sound speed for dry-air.

DISPERSION CORRECTION

There are several mechanisms which cause the propagation of sound in gases to deviate from purely adiabatic propagation. Since these mechanisms cause an increase in entropy, they lead to absorption of the wave. Also, since the non-adiabatic behavior effects the compressibility, there is dispersion, or a frequency-dependent speed of sound. Several of the known mechanisms are unimportant for the frequencies used in sound ranging, however, relaxation of the vibrational specific heats is important.

The so-called classical dispersion, due to viscosity and heat conduction, includes, for air, rotational relaxation also. This dispersion has been measured by Greenspan[10]. For frequencies below several hundred MHz, the dispersion depends on the square of the frequency and introduces a positive correction term which is smaller than the uncertainty in the gas constant for frequencies less than 5 MHz. Therefore, this effect is negligible for sound ranging.

The effect of heat radiation is to tend to make the propagation closer to isothermal (a negative correction). The important parameter is q/ω, where q is the constant used for Newton's law of cooling to describe the radiation transfer and ω is the angular frequency of the wave. When q/ω is small the propagation is close to adiabatic and when it is large, the propagation is close to isothermal. For constant q, it is clear that heat radiation is important at low frequencies. However, P. W. Smith, Jr.[11] has shown that q is not independent of ω and, further, that the maximum possible value of q/ω is 2.2×10^{-5} (q has dimensions of sec^{-1}). Since this leads to a change in speed of about 1 part in 10^{10} at the most, heat radiation is negligible for all

frequencies.

Vibrational relaxation is a different matter. Since a large number of collisions are normally required to establish vibrational energy equlibrium, high-frequency sound will not allow the vibrational energy to follow the temperature variation of the sound wave, whereas low-frequency sound will allow the establishment of equlibrium. Therefore the effective specific heats are functions of frequency and thus so is the sound speed. At very high frequencies the vibrational specific heat is "frozen" out, leading to the sound speed previously calculated c_∞. In the other extreme, for very low frequencies the sound speed is c_o where the vibrational specific heats participate. The separation of frequency regimes is characterized by the relaxation frequency f_o of the process.

In air this phenomenon is complicated by the presence of several modes of vibration which are coupled by vibrational quantum exchange. The reaction rates for the various collision partners and a normal-mode solution are required to determine the relaxation frequencies[12]. Although this has been done for moist air at room temperature[13,14] (five modes of vibration and 24 reaction rates), there are uncertainties in some of the reaction rates which effect the dispersion for low humidities (and thus dispersion in the sound ranging frequency range). In addition, the temperature dependence of some of the more important reaction rates is not well known. Nevertheless, 20°C calculations[14] show that there are three important normal modes whose strengths correspond approximately to the N_2, O_2, and CO_2 vibrational specific heats. Furthermore, it is the opinion of Sutherland[9] that, for high humidities, the H_2O vibrational specific heat relaxes with the O_2 mode, rather than separately. (They are

connected through the near-resonance transfer of vibrational energy.) Thus, to a first approximation, one may treat the case of moist air as composed of three vibrational specific heats with separate relaxation frequencies more-or-less determined by N_2-H_2O relaxation, O_2-H_2O relaxation, and CO_2-H_2O relaxation.

Under these assumptions[14],

$$\left(\frac{c_\infty}{c}\right)^2 = 1 + \sum \frac{A_i}{1+(f/f_i)^2} \quad , \tag{38}$$

where

$$A_i = k_i/k_\infty \quad , \tag{39}$$

and k_i = adiabatic compressibility of the ith mode, k_∞ = high-frequency adiabatic compressibility, f_i = relaxation frequency of the ith mode, and the sum is over 1 = N_2, 2 = O_2+H_2O, and 3 = CO_2 modes. In addition, $\Sigma k_i = k_o - k_\infty$, the difference between the low-frequency and high-frequency adiabatic compressibilities. Thus

$$\Sigma A_i = \frac{k_o}{k_\infty} - 1 = \frac{C'R}{C_v^\infty (C_p^\infty + C')} \quad , \tag{40}$$

where C' is the total vibrational molar heat capacity. Under the assumption that $C' << C_p^\infty$, this becomes

$$\Sigma A_i = \frac{R}{C_v^\infty C_p^\infty} \Sigma C_i \quad , \tag{41}$$

or

$$A_i = \frac{RC_i}{C_v^\infty C_p^\infty} \quad , \tag{42}$$

where C_i is the net contribution to the vibrational molar heat capacity due

to the ith mode

The first approximation to C_i is given by the Einstein specific heat equation

$$\frac{C_i}{R} = \Sigma\, x_j\, g_j\, u_j^2\, \frac{\exp(-u_j)}{[1-\exp(-u_j)^2]}\,, \tag{43}$$

where x_j is the mole fraction, g_j is the degeneracy, $u_j = \Theta_j/T$, and Θ_j is the vibrational characteristic temperature (the Plank-energy of the oscillator expressed in Kelvin). The sum is over all vibrational modes that participate in one of the three vibrational specific heat modes. The values for air are:

1) N_2 mode

   $x_1 = .7809\ (1-x)$

   $g_1 = 1$

   $\Theta_1 = 335$ K

2) $O_2 - H_2O$ mode

   $x_1 = .2095\ (1-x)$, $x_2 = x$

   $g_1 = g_2 = 1$

   $\Theta_1 = 2239.1$ K, $\Theta_2 = 2294.7$ K

3) CO_2 mode

   $x_1 = x_2 = x_3 = 0.0003\ (1-x)$

   $g_1 = g_3 = 1$, $g_2 = 2$

   $\Theta_1 = 1997.4$ K, $\Theta_2 = 960.3$ K, $\Theta_3 = 3380.1$ K.

In addition, there are correction terms:[15] (1) interaction between rotation and vibration (centripetal stretch), important at low temperatures, and (2) non-harmonic oscillator terms, important at high temperatures. According to tables of values presented in Hilsenrath, et al.[16] these correction

terms may be expressed by the following regressions:

N_2 contribution to air:

$$\frac{C''}{R} = (1-x)(-0.8 \times 10^{-4} + 3.5 \times 10^{-6}T), \tag{44}$$

O_2 contribution to air:

$$\frac{C''}{R} = (1-x)(-1.9 \times 10^{-4} + 2.4 \times 10^{-6}T), \tag{45}$$

H_2O contribution to air:

$$\frac{C''}{R} = x\,(-27.4 \times 10^{-4} + 78.9 \times 10^{-6}T - 1.04 \times 10^{-7}T^2), \tag{46}$$

where C'' is the correction to the molar heat capacity.

The various A_j's are plotted vs. temperature in Fig. 5, for both dry air and air at one atmosphere saturated with water vapor. The plot is actually of $-A_i/2$, since

$$c_o = c_\infty\,(1 - \tfrac{1}{2}\Sigma A_i), \tag{47}$$

where c_o is the low-frequency sound speed. Since the scale of Fig. 5 is the same as that of Fig. 2, it is clear that the dispersion corrections are of the same order as the real-gas corrections.

The actual velocity of sound is a function of frequency,

$$c = c_\infty \left(1 - (1/2)\Sigma \frac{A_i}{1 + (f/f_i)^2}\right), \tag{48}$$

where f_i are the relaxation frequencies. The frequencies have been approximated by Sutherland[9] as

$$f_n = p^* \left(\frac{293}{T}\right) [9 + 3.5 \times 10^4 x \exp(3.8 - 25/T^{1/3})], \tag{49}$$

and

$$f_o = p^* \left(\frac{293}{T}\right)^{1/2} \left[24 + 4.41 \times 10^6 x \left(\frac{5 \times 10^{-4} + x}{3.91 \times 10^{-3} + x}\right)\right], \tag{50}$$

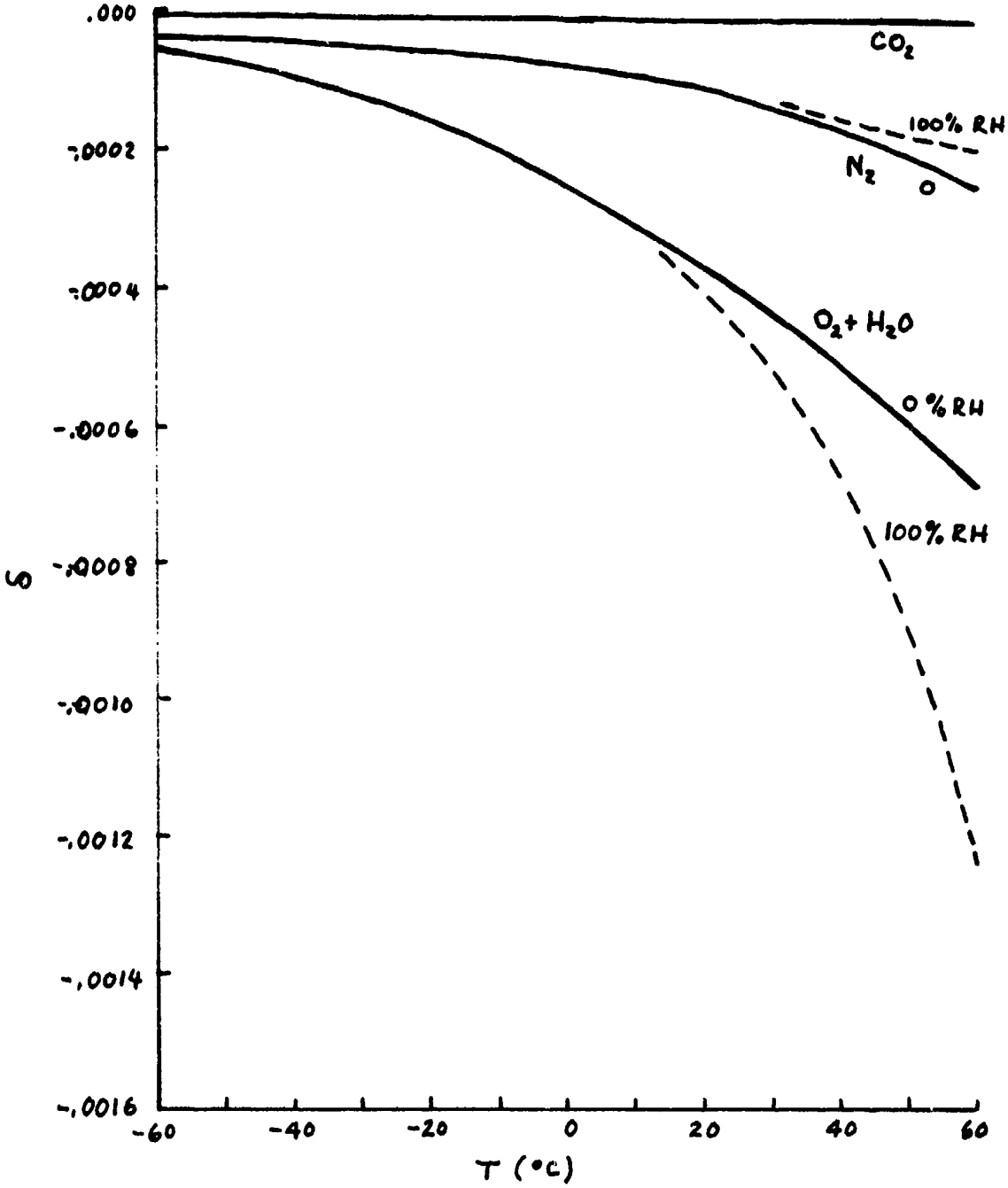

Figure 5. Contributions of Vibrational Specific Heats to the sound speed vs. temperature.

where n is for N_2 and o is for O_2-H_2O. The p^* (293/T) term is the density correction. Additional temperature corrections are the $\exp(-25/T^{1/3})$ term for the N_2-H_2O relaxation and the $(293/T)^{1/2}$ term for the O_2-H_2O relaxation. The terms independent of x in Eq. (49) and (50) are due to the CO_2 de-excitation of N_2 and O_2.

Since low frequen ies are of interest in sound ranging, some idea of the temperature dependence of CO_2 terms would be helpful. Table 5 lists some recent determinations of relaxation times for various CO_2 collisions. These data are also plotted in Fig. 6, where log $(1/\tau)$ is plotted vs. $T^{-1/3}$ (a Landau - Teller plot), the predicted major temperature dependence for exchange of vibrational energy[6]. The de-excitation of N_2 by CO_2,

$$N_2^* + CO_2 \rightarrow N_2 + CO_2 \qquad (51)$$

has been measured from 368 to 476 K. Fig. 6 indicates that the temperature dependence of this reaction is $\exp(-87/T^{1/3})$. The 9 Hz term in Sutherland's report apparently comes from 0.0003 CO_2 using the Henderson, et al. data point. If this be true, consideration of the temperature dependence indicated by Fig. 6 requires this value to be lowered.*

---

*The near-resonance between N_2 and $Co_2(\nu_3)$ suggests that the relaxation route for N_2^*-CO_2 collisions is $N_2^* + CO_2 \rightarrow N_2 + CO_2^*$ (ν_3) followed by CO_2^* $(\nu_3) + M \rightarrow CO_2^*$ $(\nu_2) + M$ and CO_2^* $(\nu_2) + M \rightarrow CO_2 + M$. Fig. 6 indicates that the over-all rate is somewhat slower than CO_2^* $(\nu_2) + M \rightarrow CO_2 + M$, which would be the controlling rate for a fast quantum exchange. Bass and Hottman (Ref. 33) have recently measured the quantum exchange at 200K, finding it about two orders of magnitude faster than the relaxation of CO_2^* (ν_3) to CO_2^* (ν_2) due to CO_2 or N_2 collisions.

Table 5. Recent determinations of relaxation times due to CO_2 collisions.

Ref.	T(K)	$1/\tau$	$T^{-1/3}$	$\ln(T/293\tau)$
		$N_2^* + CO_2 \rightarrow N_2 + CO_2$		
a	476	1.8×10^5	.128	12.6
b	448	1.9×10^5	.131	12
c	368	1.0×10^5	.140	11.7
		$O_2^* + CO_2 \rightarrow O_2 + CO_2^*$		
d	300	1.6×10^5	.149	12.0
	450	2.1×10^5	.130	12.7
	600	2.5×10^5	.119	13.1
		$CO_2^* + N_2 \rightarrow CO_2 + N_2$		
e	300	$.8 \times 10^5$	.149	11.4
	600	5×10^5	.119	13.8
		$CO_2^* + O_2 \rightarrow CO_2 + O_2$		
d	300	1.1×10^5	.149	11.6
	450	3.2×10^5	.130	13.1
	600	6.5×10^5	.119	14.1

a. Henderson, 4th International Congress on Acoustics, Copenhagen (1962)

b. Henderson,et al., J. Acoust. Soc. Am. 45, 109 (1969)

c. Bauer and Schotter, J. Chem. Phys. 51, 3261 (1969)

d. Bass, J. Chem. Phys. 58, 4783 (1973)

e. Shields, Warf, and Bass, J. Chem. Phys. 58, 3837 (1973)

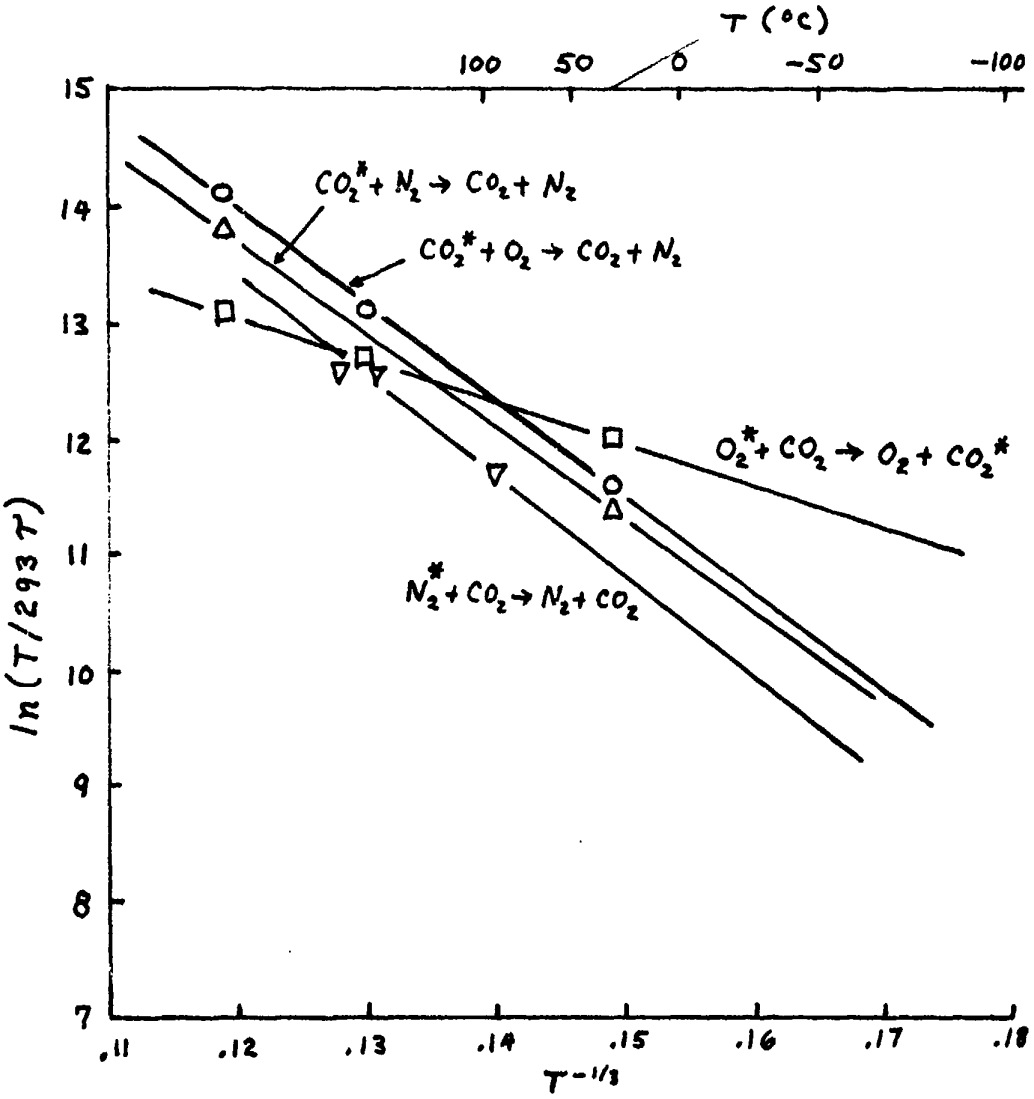

Figure 6. Temperature dependence of CO_2 - induced relaxation.

The expression used here for f_n is (52)

$$f_n = p^* \frac{293}{T} [2.3 \exp(13.1-87/T^{1/3})+3.5 \times 10^4 x \exp(3.8-25/T^{1/3})].$$

The effect of CO_2 on O_2 is supposed by Bass[17] to be controlled by the quantum exchange reaction

$$O_2^* + CO_2 \rightarrow O_2 + CO_2^* , \quad (53)$$

followed by the faster (due to the larger number of O_2 and N_2 molecules) de-excitation of CO_2 by M (O_2 or N_2)

$$CO_2^* + M \rightarrow CO_2 + M. \quad (54)$$

The temperature-dependence of reaction (53) is determined to be $\exp(-25/T^{1/3})$ from Fig. 6. Thus we will use (55)

$$f_o = 24\, p^* \frac{293}{T} \exp(5.4-25/T^{1/3}) + 4.41 \times 10^6 \left(p^*\right)\left(\frac{293}{T}\right)^{1/2} x \frac{5 \times 10^{-4} + x}{3.91 \times 10^{-3} + x} .$$

One is left with the CO_2 relaxation frequency to be determined. Calculations[14] for 20°C yield the approximately linear relation

$$f_c = 1100 + 2.0 \times 10^6 x. \quad (56)$$

The first term is due to N_2 and O_2 collisions, the measured relaxation times of which are given in Table 5 and displayed in Fig. 6, the temperature dependence of the N_2 relaxation time is $\exp(-80/T^{1/3})$, while that of O_2 is $\exp(-83/T^{1/3})$. The weighted mean of these is $\exp(-81/T^{1/3})$. The H_2O-term is due to

$$CO_2^* + H_2O \rightarrow CO_2 + H_2O \quad (57)$$

(or quantum exchange between CO_2 and H_2O). The relaxation time data for this reaction have been surveyed by Taylor and Bitterman[18]. Although there is a large spread in the data, the relaxation times seem to decrease with increasing

temperature. Taylor and Bitterman suggest as the best fit a line which has the approximate temperature dependence $\exp(27/T^{1/3})$. Thus

$$f_c = p^* \frac{293}{T} \left[1100 \exp(12.2-81/T^{1/3}) + 2.0 \times 10^6 x \exp(27/T^{1/3}-4.1)\right]. \quad (58)$$

The effect of dispersion is shown in Fig. 7, where $\delta = [c(x)-c_o]/c_o$ is plotted vs % R.H. for 20°C. For a frequency of 500 KHz, the speed is the high-frequency speed c_∞ (somewhat above c_∞^o due to real-gas effects), whereas for a frequency of 5 Hz, the speed (except at very low humidity) is the low-frequency speed of sound c_o, below c_∞ due to the additional specific heat. It is seen that for frequencies in between, the speed is intermediate. For instance, the 500-Hz speed has a rapid change from c_∞ to an intermediate speed representing O_2 equlibrium at about 4% R.H., followed by a much less rapid change toward c_o due to the N_2 relaxation at about 60% R.H.

The T-23 microphone has a frequency response from about 12 Hz to 24 Hz[19]. This suggests the receiving of 20 Hz waves; however, higher frequency components in a pulse will also cause a response. We will assume that atmospheric dispersion will separate the frequency components of a pulse over long-range propagation, thus resulting in 20-Hz reception.

For completely dry air, the relaxation frequency of CO_2 is considerably higher than 20 Hz (at least down to -60°C), the relaxation frequency of O_2 is within the bounds of the response of the microphone, and the relaxation frequency of N_2 is well below the microphone response. Since completely dry air is never found in the atmosphere, perhaps a figure of 5% R.H. is reasonable for "dry" air. In this case, the O_2 relaxation frequency falls above the range of the microphone for temperatures greater than 0°C, and the N_2 relaxation frequency is below the response for $T < 0^oC$ and above for $T > 20^oC$. For

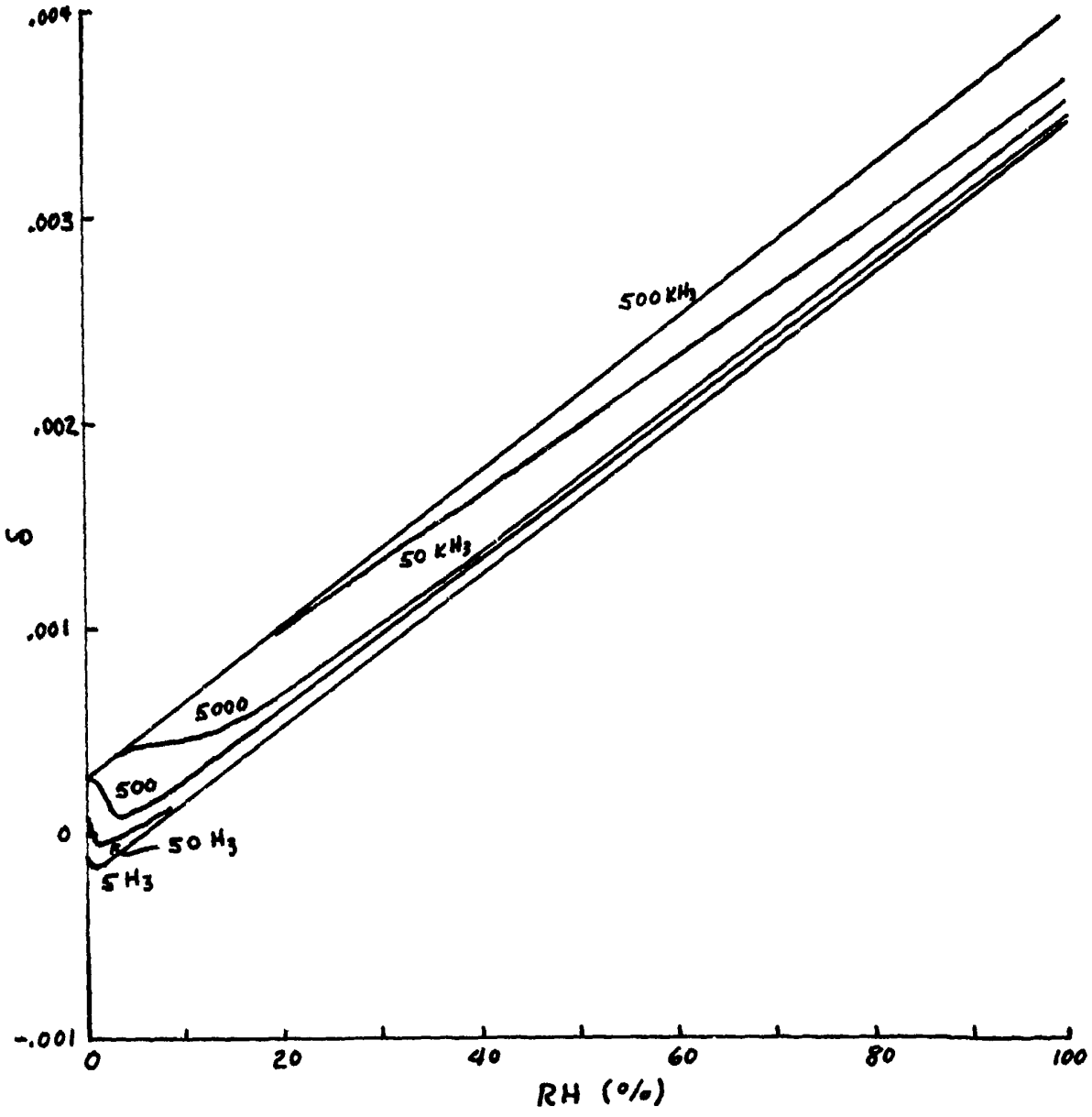

Figure 7. Dispersion for 20°C. Sound speed correction vs. % R.H.

higher humidities, the effective speed is close to c_o.

The effect of dispersion expected for sound ranging at low humidities is shown in Fig. 8, where δ is plotted vs. % R.H. for various temperatures and 20 Hz. It is clear that beyond 5% R.H. the lines are straight, with the curvature due to dispersion being largest at less than 2% R.H. Figure 9, which goes to 100% R.H., shows that the speeds are linear with humidity beyond 5% R.H.

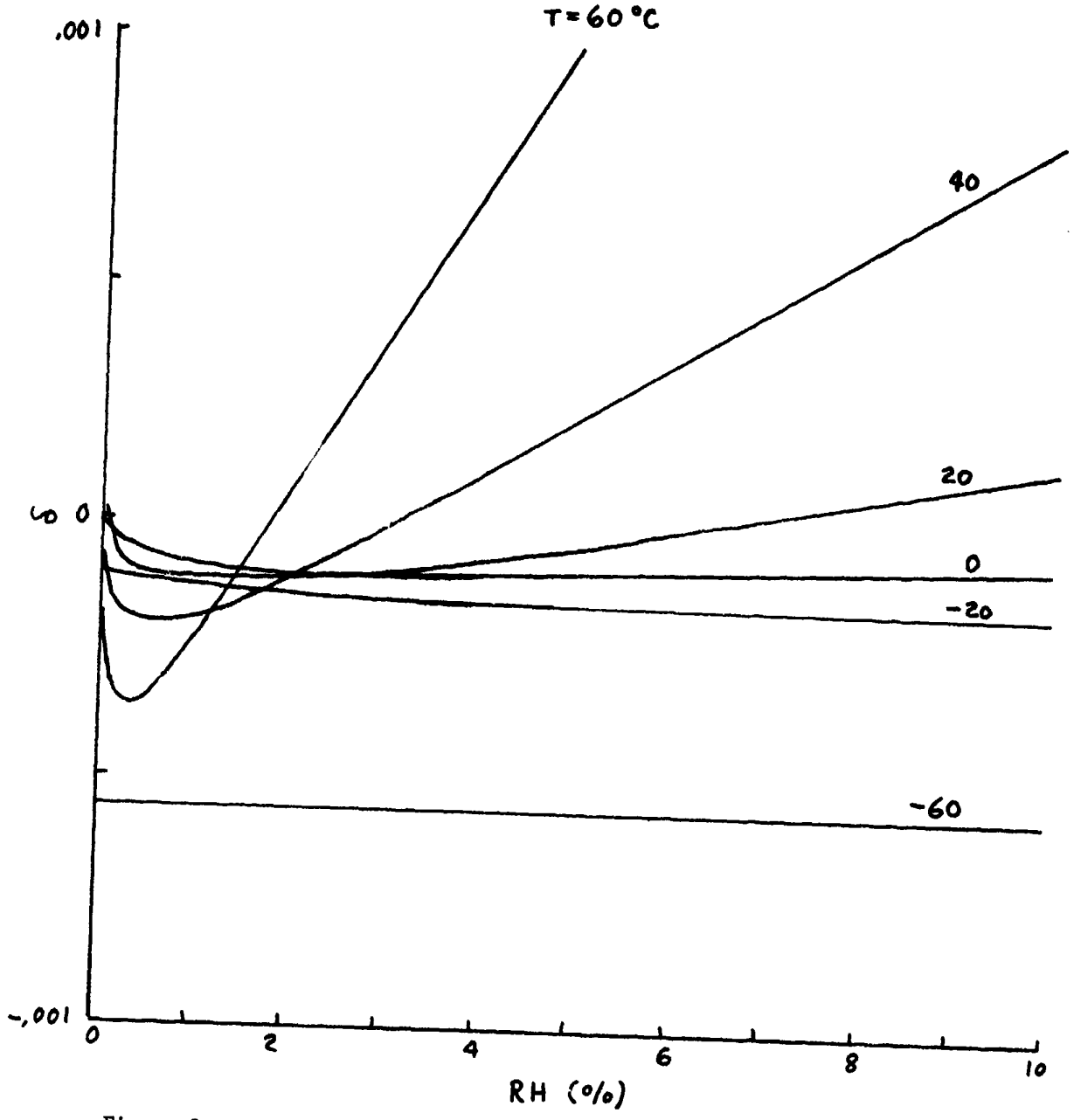

Figure 8. Sound speed correction for 20 Hz and various temperatures and low relative humidities.

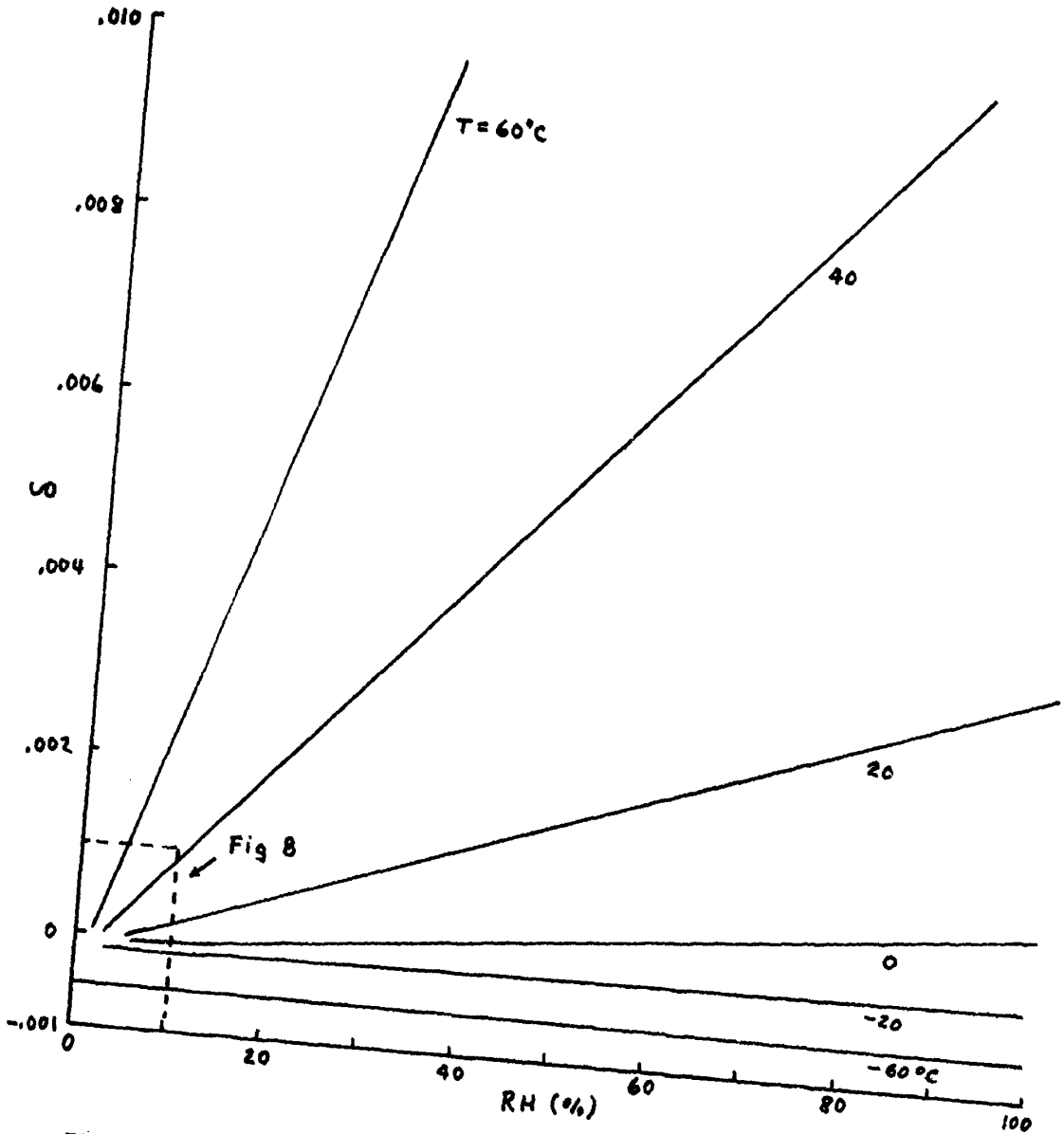

Figure 9. Sound speed correction at 20 Hz for various temperatures and relative humidities.

COMPARISON OF MODELS

The theoretical model presented above may be summarized as

$$c = 20.0577\ (T_s)^{1/2} \left\{ 1 + p^* \left(b_0 + b_1 x + b_2 x^2\right) - \sum_{i=1}^{3} d_i / [1 + (f/f_i)^2] \right\}, \quad (59)$$

where

$$b_o = 0.445/T - 76.7/T^2 - 8950/T^3, \quad (33)$$

$$b_1 = -0.481/T, \quad (34)$$

$$b_2 = -\frac{.01219}{T} \exp(1.91 + 960/T + 1.77 \times 10^5/T^2), \quad (35)$$

$$d_1 = (1-x)(-9.9 \times 10^{-4} + 1.43 \times 10^{-5}T - 6.68 \times 10^{-8}T^2 + 1.05 \times 10^{-10}T^3), \quad (60)$$

$$d_2 = 4.9 \times 10^{-4} - 4.1 \times 10^{-6}T + 1.7 \times 10^{-9}T^2 + 3.7 \times 10^{-11}T^3 + x(1.07 \times 10^{-3} - 3.4 \times 10^{-6}T - 2.96 \times 10^{-8}T^2 + 1.65 \times 10^{-10}T^3), \quad (61)$$

$$d_3 = -1 \times 10^{-5} + 1 \times 10^{-7}T, \quad (62)$$

$$f_1 = p^*[1.72 - 2.25 \times 10^{-2}T + 8.37 \times 10^{-5}T^2 + x(1.19 \times 10^4 + 125T - .1585T^2)], \quad (63)$$

$$f_2 = p^*\left[-5.2 + .133T - 1.13 \times 10^{-4}T^2 + 7.55 \times 10^7 x \frac{5 \times 10^{-4} + x}{3.91 \times 10^{-3} + x} \times (T)^{-1/2}\right], \quad (64)$$

$$f_3 = p^*[460 - 7.12T + .0318T^2 + x(1.79 \times 10^6 - 1.29 \times 10^9/T + 3.86 \times 10^{11}/T^2)], \quad (65)$$

and

$$T_s = \frac{(1+.1459x)T}{(1-.1546x - .0773x^2)}. \quad (66)$$

Equations (60)-(65) are regression fits to the more complicated equations in the dispersion section. They yield results well within the uncertainty for temperatures $-90^oC < T < 90^oC$.

The mole fraction of water vapor may be determined from the measurement of the virtual temperature or relative humidity. Using Eq. (14) and (18),

$$x = \frac{T_v - T}{.378 T_v} \quad , \tag{67}$$

or,

$$x = \frac{u x_s}{100 p^*} \quad , \tag{68}$$

where u is the % R.H. and x_s is the saturated mole fraction given by Eq. (36).

The model is subject to large extrapolations for frequencies below about 100 Hz and the exclusion of viscothermal dispersion limits the high frequency range to about 5 MHz/atm. The uncertainty in the calculations varies with temperature. Table 6 lists reasonable uncertainties due to the various effects. The real-gas errors are based on the uncertainties in Table 4. The magnitude of the specific heat was assumed to be uncertain by the amount of the N_2 vibrational-rotational correction, varying between 0.001 R at -90°C to 0.002 R at 90°C. The uncertainties due to lack of knowledge of the relaxation frequencies were determined by trial calculations at 5% R.H. The relaxation frequencies were considered to vary by ± 50% at 0°C and 30°C, ± 100% at -30°C and 60°C, and ± 200% at -90°C, -60°C, and 90°C. Zero R.H. uncertainties would be larger.

A comparison of this model with others is displayed in Fig. 10. Here the display is Δc in m/sec vs. temperature. The two values of relative humidity, 5% and 95% are dispayed. The highest curves are the present model, Eq. (1) and (2). It is seen that the low-humidity curve is consistently high and that the high-humidity curve is only within ± .05 m/sec (the dotted lines) between 15°C and 30°C, being about 0.2 m/sec low at 40°C. The more-or-less parallel

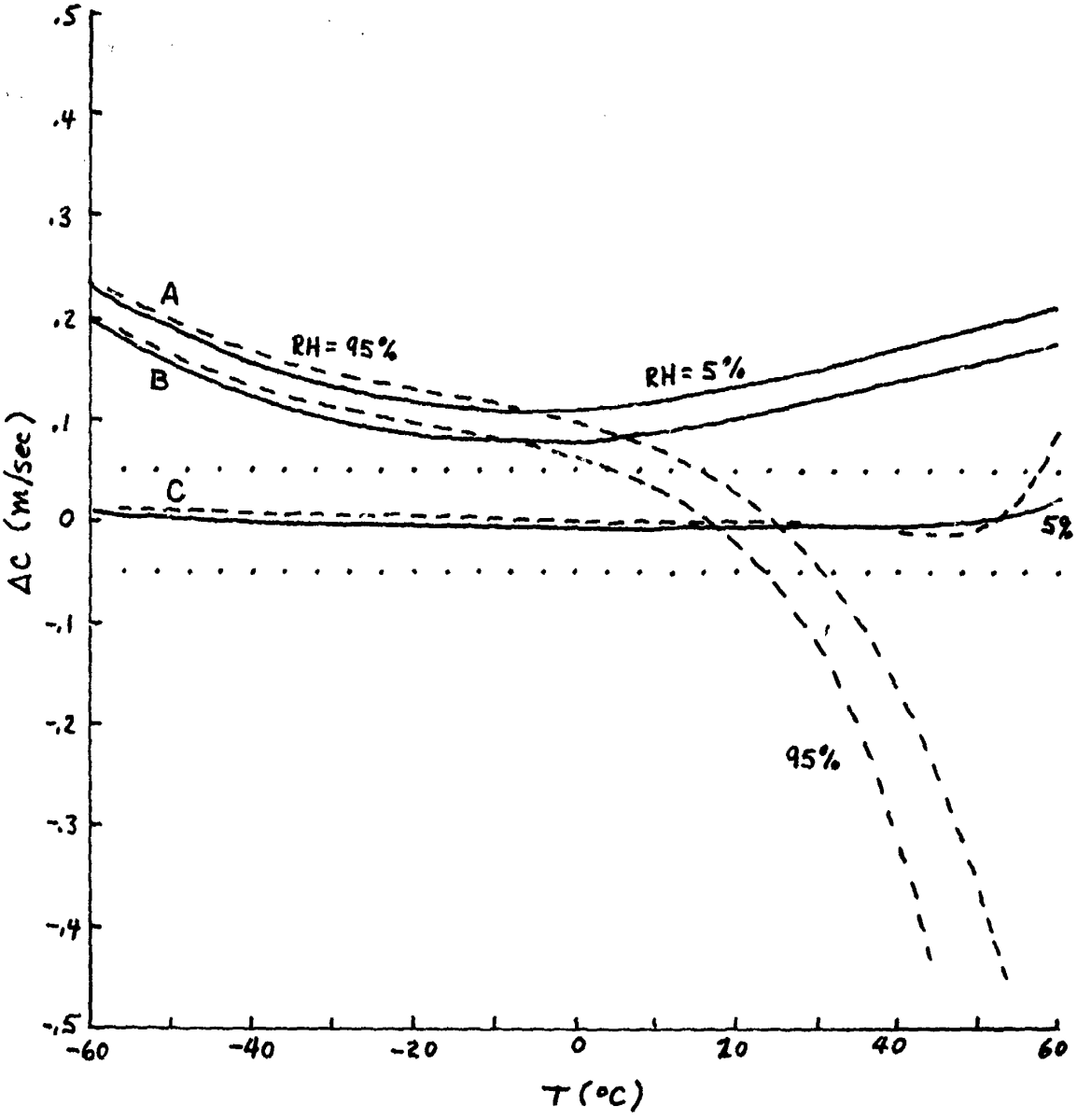

Figure 10. Differences in sound speed for various models. All models compared to theory developed in this work, with 5% and 95% R.H. calculations displayed. A: Present sound-ranging method. B: Gutenberg's formula. C: Regression fit good below 50°C.

Table 6. Uncertainties in the theoretical calculation of sound speed. IG represents that due to the ideal-gas speed, RG represents that due to the equation of state correction at one atmosphere, CV represents that due to calculations of the vibrational specific heat terms, and RF is due to supposed errors in the relaxation frequencies.

T	ERROR (m/sec)				
(^{o}c)	IG	RG	CV	RF	TOTAL
-90	0.01	0.21	0.01	0.01	0.21
-60	0.01	0.11	0.01	0.02	0.11
-30	0.01	0.07	0.02	0.02	0.07
0	0.01	0.05	0.02	0.01	0.05
30	0.01	0.03	0.02	0.01	0.04
60	0.01	0.02	0.02	0.01	0.04
90	0.01	0.02	0.03	0.01	0.04

curves are due to Gutenberg (see Eq. (15)). The humidity correction of the present model is somewhat better than Gutenberg's, while the use of 273.2 rather than 273.15 for the ice point causes the parallel displacement. Also shown in Fig. 10 is a regression fit to Eq. (59) which is accurate below 50^{o}C and is represented by

$$c = 20.0577\ (1 + A + xB)\ \sqrt{T}\ , \tag{69}$$

where

$$A = -1.43 \times 10^{-4} - 1.34 \times 10^{-6} T - 1.118 \times 10^{-7} T^2 + 3.03 \times 10^{-10} T^3\ , \tag{70}$$

$$B = .1516 + 5.86 \times 10^{-4} T - 1.793 \times 10^{-5} T^2 + 2.00 \times 10^{-7} \times T^3. \tag{71}$$

Although this takes less than 1/10 calculator time than Eq. (59), it can be seen to agree within less than .01 m/sec below 50^{o}C. This regression, however, does not agree with Eq. (59) for very low humidities (<3% R.H.). The slope of c vs x (Eq. 71) was determined by least-squares fitting the humidity points

every 10% from 5% to 95%, and does not include the dispersion "loops" shown in Fig. 8. The intercepts of these linear fits (Eq. 70) and the slopes were fitted with a cubic in T between $-50^{o}C$ and $50^{o}C$. The deviation beyond $50^{o}C$ is clear in Fig. 10.

The shift between the present model and Gutenberg's suggests that the present model can be improved by lowering the effective temperature and raising the % of virtual temperature used. The results of such a simple change are shown in Fig. 11. A constant 0.2^{o} was subtracted from the "sonic" temperature and 80% rather than 75% of the virtual temperature was used to obtain this plot. It is seen to be within ± .05 m/sec of theory between $-40^{o}C$ and $30^{o}C$ (for 5% R.H.), with 50% R.H. values being within this range beyond $60^{o}C$. The 80% figure was chosen because it allowed the 50% R.H. curve to be flat. Thus the value

$$T_s = t + .8\Delta t + 273.0 \ , \tag{72}$$

where Δt is the difference between the virtual temperature and the dry-bulb temperature, is within ± 0.05 m/sec of about 90% of expected sound-ranging weather.

One can, with small additional temperature corrections, do better. A quadratic temperature correction to straighten the 5% curve, a small tilt of the resulting 5% curve and the use of 82 1/2% of the virtual temperature results in Fig. 12. Here

$$T_s = t - 1 \times 10^{-3}t - 6 \times 10^{-5}t^2 + .825\Delta t + 273.0 \ . \tag{73}$$

It is noted that this correction is almost as good as Eq. (69) but it only involves a quadratic for A, and B is constant.

The effect of pressure on the speed of sound is depicted in Fig. 13.

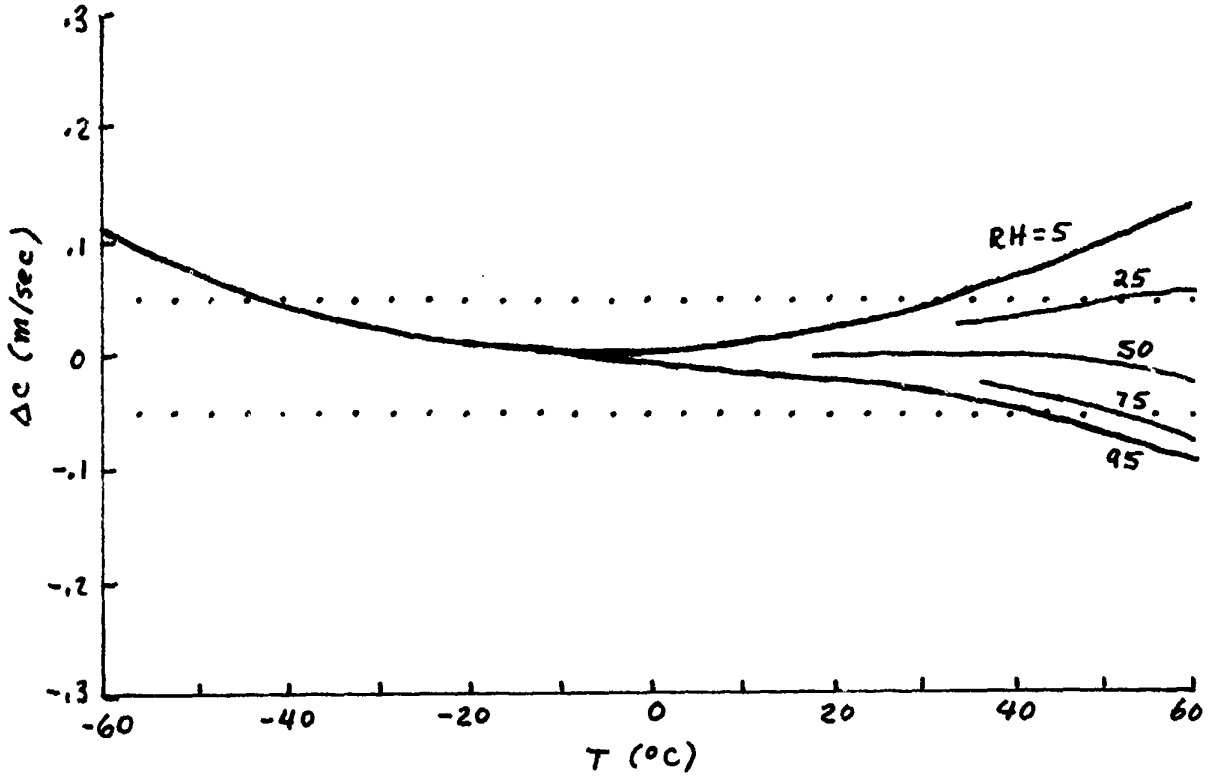

Figure 11. Difference between theory and $c = 20.06\sqrt{T_s}$ where $T_s = t + .8\Delta t + 273.0$. Various relative humidities are shown for the higher temperatures.

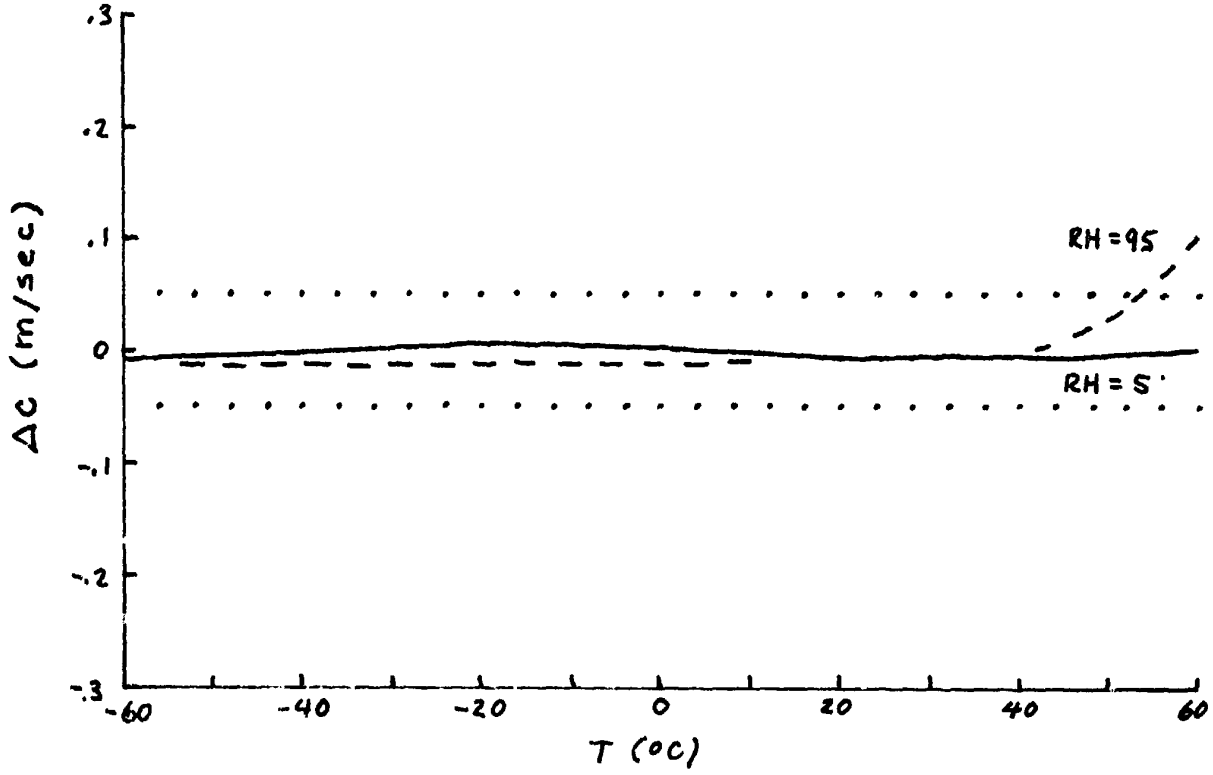

Figure 12. Difference between theory and $c = 20.06\sqrt{T_s}$, where $T_s = t + .825\Delta t - 1 \times 10^{-3}t - 6 \times 10^{-5}t^2 + 273.0$.

Here the 50% R.H. curve calculated from Eq. (73) is plotted for 0.7 and 1 atm. It is seen that even for 0.7 atm, the curve is still within ± .05 m/sec. The effect of dispersion errors are shown in Fig. 14, where the 50% R.H. curve calculated from Eq. (73) is plotted vs the sound speed for 0.2, 20, and 2000 Hz. Again, over this large range of frequency, the approximation falls within ± 0.05 m/sec of theory.

The same insensitivity to frequency does not hold at low humidities. Fig. 15 shows that the calculated speed using Eq. (73) is about 0.1 m/sec low for 2000 Hz sound at 10°C and 5% R.H. At that temperature and humidity, the O_2 begins to relax and the speeds calculated for higher temperatures are better. The dashed line represents the difference between the model and the 0% R.H. 2000-Hz speed, being about 0.3 m/sec below the model at 60°C (this is the total dispersion difference between c_o and c_∞).

Except for these very low humidities, it is observed that simple corrections to the present model for sound speed will agree to within ± 0.05 m/sec of the more detailed model over the range of temperature and pressure expected in sound ranging.

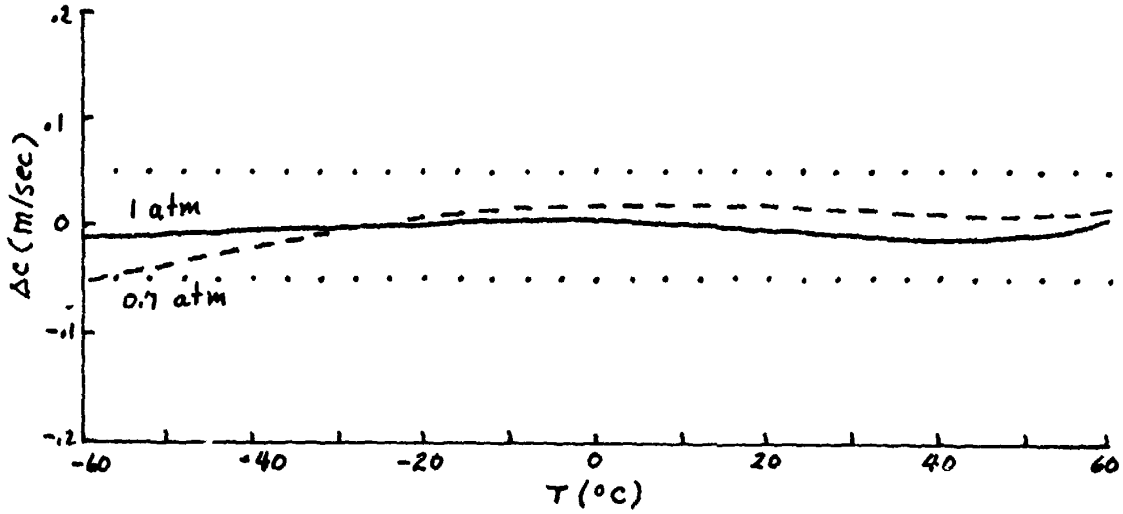

Figure 13. Difference between theory and approximation given by Eq. (1) and Eq. (73). Relative humidity = 50%, pressure = 1 and 0.7 atm.

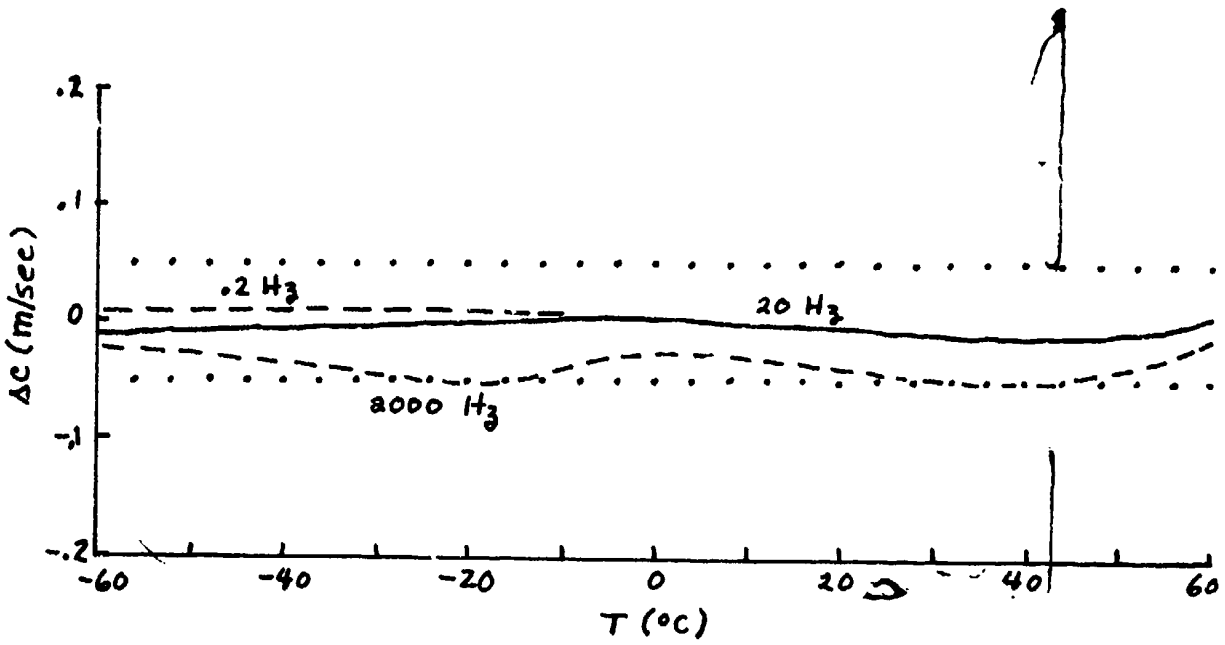

Figure 14. Difference between theory and approximation given by Eq. (1) and (73). Effec dispersion curves for frequencies of 0.2, 20, and 2000 Hz and rel ve humidity of 50%.

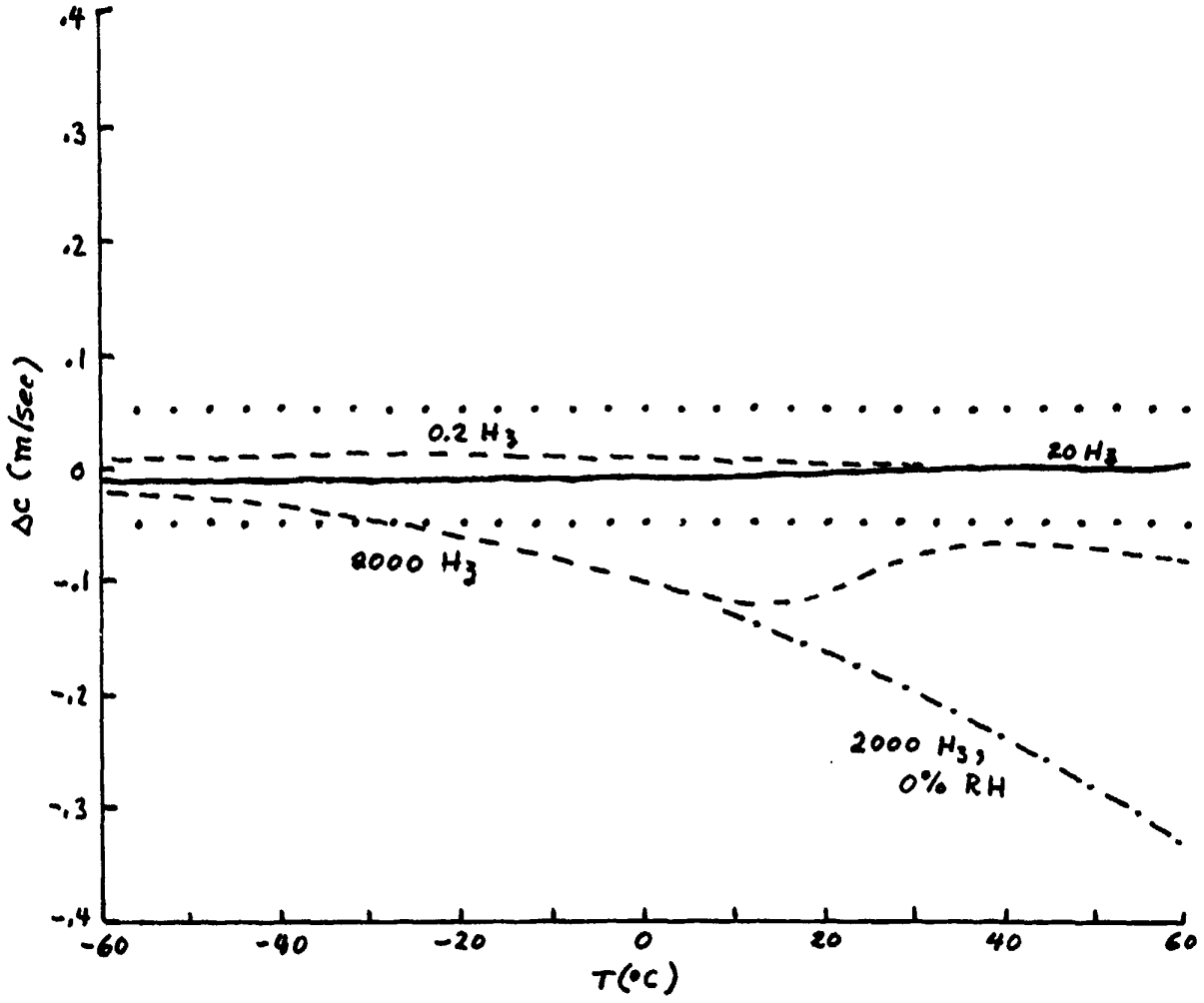

Figure 15. Difference between theory and approximation given by Eq. (1) and (73). Effect of dispersion at 5% R.H. Dotted curve is for 0% R.H.

EXPERIMENTAL RESULTS

Most speed of sound measurements in air were taken previous to World War II. Open-air measurements are beset with temperature and wind difficulties. Laboratory measurements allow the control of temperature and humidity. Data taken at specific temperatures are reduced to a near-by standard temperature such as $0^{o}C$ or $20^{o}C$ by the use of ideal-gas temperature dependence. After the discovery of dispersion, reduction to low-frequency speeds was sometimes done, since most measurements were in the MHz range.

Hardy, Telfair, and Pielemeier[20] obtained 331.44 ± .05 m/sec reduced to c_o at $0^{o}C$. Their survey of results up to 1942 yielded a weighted mean of 331.46 ± .05 m/sec. The theoretical results detailed above are in agreement with these values, yielding 331.44 ± .05 m/sec. Equation (1) yields 331.57 m/sec.

Several investigators have measured both high-frequency (several MHz) and low-frequency (200 Hz-2000 Hz) for $20^{o}C$ with varying amounts of water vapor. These results, along with theoretical curves for c_∞ and c_o are shown in Fig. 16. The open data points represent data taken at high frequencies, whereas the +, x, and * represent low-frequency measurements. The estimated uncertainties on individual data points lie in the region of ± .1 m/sec. There is excellent agreement between theory and both sets of data. Harris' data (+) were not reported as absolute, only relative. In plotting these data, his 0% humidity value was assumed to be equal to the c_∞ value for dry air. According to Fig. 7, as the humidity increases, the data should fall to the c_o curve. Although there is some overshoot, the data seem to do this, a fact pointed out by Harris[21].

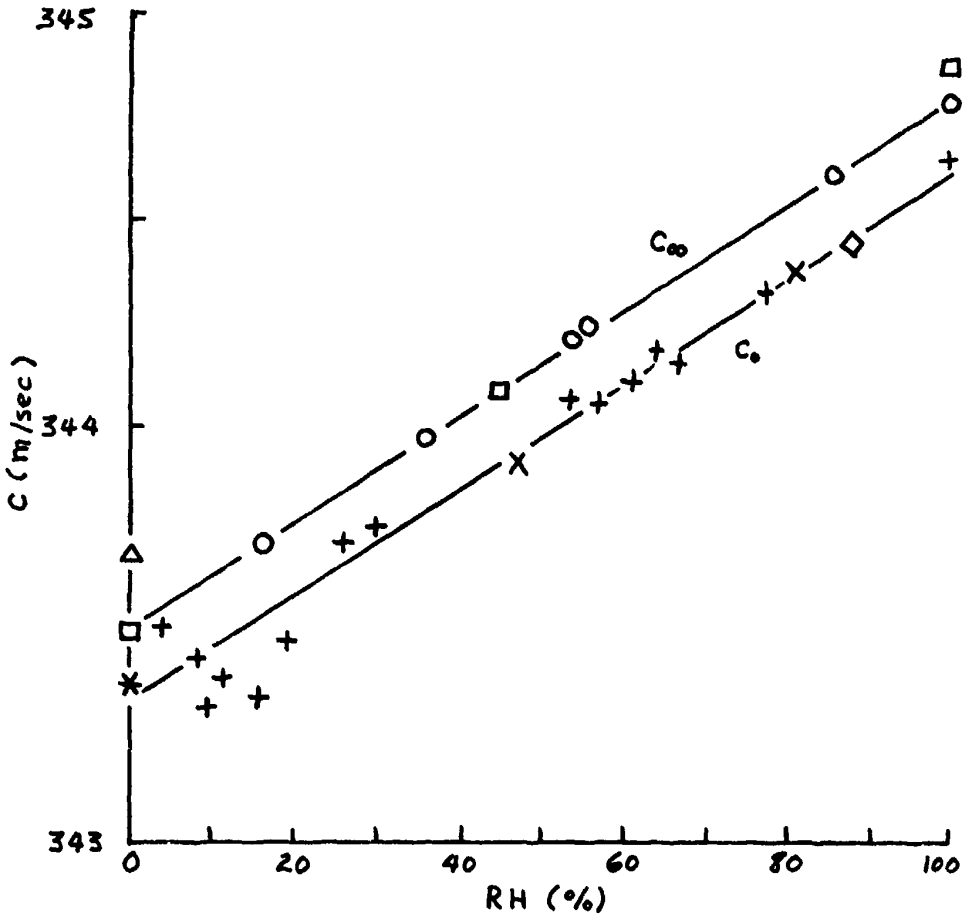

Figure 16. Experimental results for sound speed in humid air at 20°C. High frequency data: □ Reid, Phys. Rev. 35, 814(1930); ◊ Grabau, J. Acoust. Soc. Am. 5, 1(1933); Δ Norton, J. Acoust. Soc. Am. 7, 16(1935); O Pielemeier, J. Acoust. Soc. Am. 10, 313(1939). Low-frequency data: X Hebb, Phys. Rev. 20, 89(1905) and Phys. Rev. 14, 74(1919); * Partington and Shilling, Phil. Mag. 6, 920(1928); + Harris, J. Acoust. Soc. Am. 49, 890(1971).

Pielemeier[22] has also reported data taken at 30°C, where air will hold more water vapor and the separation between c_o and c_∞ is greater. His data are shown in Fig. 17. The data were corrected for a systematic error he later reported[20]. This data shows good agreement with the c_∞ theory.

Results for wide ranges of temperature are lacking for air. However, for various pure gases, speed of sound measurements have been made over wide ranges of temperature and pressure. For example, Gammon[23] has measured the speed of sound in helium (where there is no vibrational dispersion) from -175°C to 150°C and from 10 atm to 50 atm of pressure. His data clearly show that the real-gas effect is linear for pressures in the order of one atm. When the sound of speed is extrapolated to zero pressure, his data also indicate that the deviation of the ideal-gas sound speed from $\sqrt{T}$ dependence is within about 30 ppm over this range of temperature, with some of this deviation possibly due to inaccuracy in measuring the temperature.

It may be concluded that experimental results show no evidence of inadequacies in the theory of the speed of sound in gases. In fact, measurements of sound speed are as accurate determinations of the gas constant, temperature, and the ratio of specific heats as competing methods. The only problem for air seems to be the determination of vibrational relaxation times.

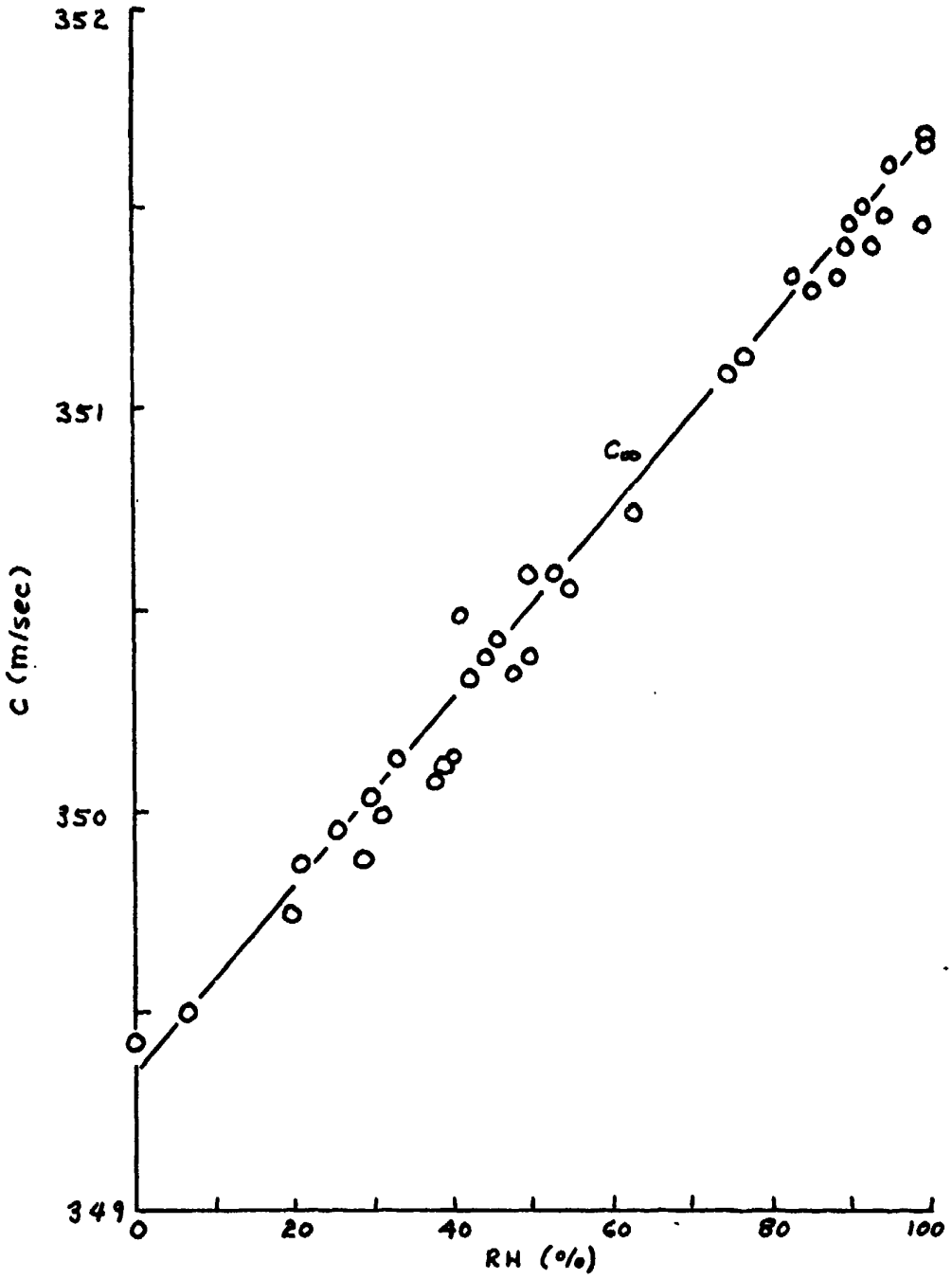

Figure 17. Experimental results for the speed of sound in humid air at 30°C. Pielemeier, J. Acoust. Soc. Am. 10, 313(1939).

OTHER ATMOSPHERIC EFFECTS

Sound ranging involves propagation of signals that over part of their path have excess pressures that are not negligible compared to the ambient pressure. In addition, the propagation includes refraction and/or reflection from the ground. Furthermore, the atmosphere differs from a simple mixture of gases in a laboratory bottle. Some of these phenomena affect the speed of the signal.

For a finite-amplitude signal, the speed of propagation is[24]

$$c = c_o + \frac{\gamma-1}{2} u, \tag{74}$$

where u is the acoustic "particle" velocity. Since $u = p/\rho c$, where p is the acoustic overpressure, positive-pressure parts of a signal travel faster than the small-signal speed of sound. Unlike water waves, acoustic waves can't "break", and the propagation becomes that of a shock wave. The treatment in this study is restricted to small-signal waves: any finite-amplitude corrections to the sound speed must be treated separately.

The refraction of sound follows Fermat's principle and takes the path of least time[25]. The addition of wind complicates the determination of this path, however, we assume that an effective temperature and wind are available for the solution of the sound ranging problem. Thus one is left with the problem of determining the effective sound speed from the effective temperature, which is the concern of this work.*

---

*Finite amplitude and refraction effects on the speed of sound for sound ranging purposes are treated in reference 32.

Due to both the source and receiver being close to the ground, sound ranging involves direct, reflected, ground, and surface waves close to the air-ground boundary. This type of propagation has been investigated by Embleton, et al.[26], with the result that, although the amplitude of the signal is affected, the speed of sound is independent of such complications.

Even an isothermal, non-moving atmosphere has a vertical density gradient due to gravity. Some years ago Bergmann[27] showed that such a situation leads to dispersion:

$$c = c_o \left(1 - \frac{n}{2\pi\lambda^2}\right) , \tag{75}$$

where

$$n = \frac{1}{2\rho} \nabla^2\rho - \frac{3}{4} \left(\frac{\nabla\rho}{\rho}\right)^2 . \tag{76}$$

For an isothermal atmosphere, the density profile is

$$\rho(z) = \rho_o \exp(-z/H), \tag{77}$$

where z is the altitude, H = RT/gM (the scale height), and where g is the acceleration due to gravity. This leads to $n = (5/4)/H^2$, or using H = 8 km,

$$c = c_o(1 - 2.6 \times 10^{-5}/f^2) . \tag{78}$$

Thus the dispersion is only important for frequencies less than 1 Hz (wavelengths on the order of the scale height).

Turbulence introduces dispersion also. Wenzel[28] has shown that the speed is reduced by a factor on the order of $\langle(\Delta c/c)^2\rangle$, where $\langle(\Delta c/c)^2\rangle$ is the mean square fluctuation in sound speed over a region on the order of a wavelength or less. An estimate of this effect is that for a value of $\Delta T = 1^oC$, the factor is on the order of 3 ppm, and for $\Delta v = 1$ m/sec, the factor is on the order of 10 ppm. The value $\Delta v = 1$ m/sec is probably a useful upper bound since

this much wind fluctuation would create quite a bit of noise. For instance, using Bernoulli's principle, the variation in pressure due to wind fluctuations should be on the order of $\Delta p = \rho v \Delta v$, or 130 dyne/cm^2 for a wind of v = 10 m/sec with Δv = 1m/sec. This would probably put the sound ranger out of business. Thus turbulent dispersion is neglected.

Small aerosol particles may be assumed to be in Boltzmann equilibrium with the air molecules, thus acting like huge molecules, increasing the mean molecular mass. According to Junge's[29] size distribution of aerosols, the major effect should come from particles in the 0.1 to 1μm range (about 1000 per cm^3). Assuming a mean density of 2.5 gm/cm^3, the effect of particles in this range is to increase the mean molar mass by about 10^{-4} amu, less than the uncertainty in M due to CO_2 variation.

Finally, the effect of fogs is quite complicated, but has been treated by the introduction of the water droplets as a third gas along with water vapor and dry air. The result is a relaxation process involving viscothermal, mass, and latent heat transfer between the liquid and vapor phases of water. Davidson[30] finds that the dispersion due to fogs is only important below 1 Hz.

Thus the atmosphere apparently introduces no speed of sound effects (above 1 Hz) that can't be measured in the laboratory. Refraction and finite-amplitude effects on sound-ranging effective speeds must, however, be accounted for separately as effective temperatures and Mach numbers.

SUMMARY AND RECOMMENDATIONS

A model for the speed of sound in air which includes the real-gas effects of humid air and vibrational dispersion has been investigated. Other effects such as dispersion due to rotational relaxation, heat radiation, density gradients, boundary propagation, turbulence, aerosols, and fogs were considered and found to be unimportant for the frequencies of interest in sound ranging. The uncertainty in predicting the sound speed is estimated to vary between ± 0.08 m/sec at -40°C, ± .05 m/sec at 0°C, and ± 0.04 m/sec at 40°C. Experimental results in humid air at 20°C and 30°C are in excellent agreement with the model.

The present method of determining the sound speed for sound ranging purposes differs from this model by about + .2 m/sec at -40°C, and by about + .2 m/sec (5% R.H.) and -.2 m/sec (95% R.H.) at 40°C. The present model is about .1 m/sec high at the standard sound-ranging temperature of 10°C.

If the present formula for "sonic" temperature,

$$T_s = \frac{3t_v + t}{4} + 273.2 \quad , \tag{2}$$

is modified to

$$T_s = .825t_v + .174t + 273.0 - 6 \times 10^{-5}t^2 \quad , \tag{73}$$

then the predicted sound speed will fall within ± 0.05 m/sec of the theory between -60°C and 50°C for relative humidities greater than about 3%. There is no need for pressure corrections down to pressures of 0.7 atm. And, unless the relaxation frequencies are off by factors of 50, dispersion results will be within ± .05 m/sec for humidities greater than 5% R.H.

Although the difference produced by this change in evaluating the "sonic"

temperature amounts to no more than 0.2 m/sec within the temperature range from -40°C to 40°C, there are several reasons for changing the present procedure:

1) The errors in determining sound speed are systematic rather than random. An error of + .2 m/sec will always predict the source to be 60m farther away at 10 km, whereas random errors tend to cancel out over the six microphones or from signal to signal from the same source.

2) The meteorological message "sonic" temperature is rounded to the nearest tenth of a degree, implying ± .05°C, or ± .03 m/sec accuracy. Likewise, tables of sound speed in the sound ranging field manual[31] are expressed to the nearest tenth of a meter per sec. In this case, the implied accuracy is not justified.

3) The change required is in the meteorological message, not the sound ranging solution. This will simplify the implementation, since the difference in computational effort between

$$t_s = .75t_v + .25t$$

and

$$t_s = .825t_v + .174t - .2 - 6 \times 10^{-5}t^2$$

is not great for persons trained to reduce meteorological data.

It is the author's recommendation that the change in method of calculating the "sonic" temperature be considered along with other improvements in the sound ranging system.

Acknowledgement

This work was supported by Battelle Columbus Laboratories, Durham, North Carolina. The author appreciates the helpful comments of A. J. Blanco and D. M. Swingle of the Atmospheric Sciences Laboratory.

References

1. Anonymous. Artillery Meteorology. F.M. 6-15. (Department of the Army, Washington, D. C., 1970).
2. D. M. Swingle, private communication.
3. B. Gutenberg, J. Acoust. Soc. Am. 14, 151(1942).
4. B. Gutenberg, Sound propagation in the atmosphere, p. 366, Compendium of Meteorology. (Am. Meteor. Soc., Boston, 1951).
5. E. R. Cohen and B. N. Taylor, J. Phys. Chem. Ref. Data 2, 663(1973).
6. K. F. Hertzfeld and T. A. Litovitz. Absorption and Dispersion of Ultrasonic Waves. (Academic Press, New York, 1959).
7. J. O. Hirschfelder, C. F. Curtess, and R. B. Bird. The Molecular Theory of Gasses and Liquids. (John Wiley, New York, 1954).
8. J. A. Goff, Trans. A.S.H.V.E. 55, 459(1949).
9. L. C. Sutherland. Review of Experimental Data in Support of a Proposed New Method for Computing Atmospheric Absorption Losses. Dept. Trans. Rept DOT-TST-75-87(1975).
10. M. Greenspan, J. Acoust. Soc. Am. 31, 155(1959).
11. P. W. Smith, Jr., J. Acoust. Soc. Am. 29, 693(1957).
12. H.-J. Bauer, F. D. Shields, and H. E. Bass, J. Chem. Phys. 57, 4624(1972).
13. L. B. Evans, H. E. Bass, and L. C. Sutherland, J. Acoust. Soc. Am. 51, 1565(1972).
14. H. E. Bass, H.-J. Bauer, and L. B. Evans, J. Acoust. Soc. Am. 51, 821(1972).
15. N. Davidson. Statistical Mechanics. (McGraw-Hill), New York, 1962).
16. J. Hilsenrath, et al. Tables of Thermal Properties of Gases. N.B.S. Circular 564 (U.S. Gov. Printing Off., Washington, 1955).
17. H. E. Bass, J. Chem. Phys. 58, 4783(1973).
18. R. L. Taylor and S. Bitterman, Rev. Mod. Phys. 41, 26(1969).
19. E. A. Dean, J. G. Pruitt, and L. L. Chapin. Sound Ranging for the Rocket Grenade Experiment. Quarterly Prog. Rept. #1, Contract NAS 5-556. (Schellenger Research Laboratories, El Paso, 1961).
20. H. C. Hardy, D. Telfair, and W. H. Pielemeier, J. Acoust. Soc. Am. 13, 226 (1942).
21. C. M. Harris, J. Acoust. Soc. Am. 49, 890(1971).

22. W. H. Pielemeier, J. Acoust. Soc. Am. 10, 313(1939).
23. B. E. Gammon, J. Chem. Phys. 64, 2556(1976).
24. R. B. Lindsay. Mechanical Radiation. (McGraw-Hill, New York, 1960).
25. P. Ugincius, J. Acoust. Soc. Am. 51, 1759(1972).
26. T.F.W. Embleton, J. E. Piercy, and N. Olson, J. Acoust. Soc. Am. 59, 267 (1976).
27. P. G. Bergmann, J. Acoust. Soc. Am. 17, 329(1946).
28. A. R. Wenzel, J. Acoust. Soc. Am. 51, 1683(1972).
29. C. E. Junge. Air Chemistry and Radioactivity (Academic Press, New York, 1963).
30. G. A. Davidson, J. Atmos. Sci. 32, 2201(1975).
31. Anonymous. Field Artillery Sound Ranging and Flash Ranging. FM 6-122 (Department of the Army, Washington, D. C., 1979).
32. E. A. Dean. On the Determination of Arrival Times for Sound Ranging. I. Effects of Finite Amplitude Propagation, Vertical Meteorological Gradients, and System Transient Response. Rept. No. ASL-CR-79-0100-2 (Atmospheric Sciences Laboratory, White Sands Missile Range, 1979).
33. H. E. Bass and S. D. Hottman, J. Chem. Phys. 67, 5966(1977).

★ U.S.GOVERNMENT PRINTING OFFICE: 1979 — 677-017/27